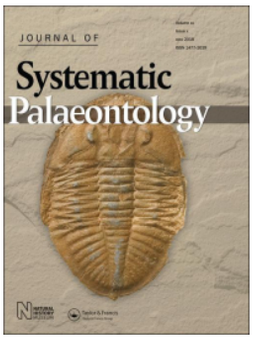

Journal of Systematic Palaeontology

ISSN: (Print) (Online) Journal homepage: www.tandfonline.com/journals/tjsp20

The postcranial skeleton of *Amphimoschus* Bourgeois, 1873 (Cetartiodactyla, Ruminantia, Pecora) sheds light on its phylogeny and the evolution of the clade Cervoidea

Israel M. Sánchez, Juan L. Cantalapiedra, Daniel DeMiguel, Beatriz Azanza, Flavia Strani & Jorge Morales

To cite this article: Israel M. Sánchez, Juan L. Cantalapiedra, Daniel DeMiguel, Beatriz Azanza, Flavia Strani & Jorge Morales (2024) The postcranial skeleton of *Amphimoschus* Bourgeois, 1873 (Cetartiodactyla, Ruminantia, Pecora) sheds light on its phylogeny and the evolution of the clade Cervoidea, Journal of Systematic Palaeontology, 22:1, 2386020, DOI: 10.1080/14772019.2024.2386020

To link to this article: https://doi.org/10.1080/14772019.2024.2386020

Journal of Systematic Palaeontology, 2024
Vol. 22, No. 1, 2386020
http://dx.doi.org/10.1080/14772019.2024.2386020

Taylor & Francis
Taylor & Francis Group

The postcranial skeleton of *Amphimoschus* Bourgeois, 1873 (Cetartiodactyla, Ruminantia, Pecora) sheds light on its phylogeny and the evolution of the clade Cervoidea

Israel M. Sánchez[a]*, Juan L. Cantalapiedra[b], Daniel DeMiguel[a,c,d], Beatriz Azanza[d], Flavia Strani[d,e] and Jorge Morales[f]

[a]*Paleodiversity & Phylogeny Research Group, Institut Català de Paleontologia Miquel Crusafont, Universitat Autònoma de Barcelona, Edifici ICTA-ICP, c/Columnes s/n, Campus de la UAB, 08193 Cerdanyola del Vallès, Barcelona, Spain;* [b]*Departamento de Ciencias de la Vida, Universidad de Alcalá, GloCEE-Global Change Ecology and Evolution Research Group, 28805, Alcalá de Henares, Madrid, Spain;* [c]*ARAID Foundation, Av. de Ranillas 1-D, planta 2*[a]*, oficina B, 50018, Zaragoza, Spain;* [d]*Universidad de Zaragoza, Departamento de Ciencias de la Tierra, and Instituto Universitario de Investigación en Ciencias Ambientales de Aragón (IUCA), Pedro Cerbuna 12, 50009 Zaragoza, Spain;* [e]*Dipartimento di Scienze della Terra, Sapienza-Universitè di Roma, 00185 Rome, Italy;* [f]*Departamento de Paleobiología, Museo Nacional de Ciencias Naturales-CSIC, C/José Gutiérrez Abascal, 2, 288006 Madrid, Spain.*

(Received 4 July 2023; accepted 22 July 2024)

Here we present the first description of the postcranial skeleton of *Amphimoschus*, an enigmatic hornless ruminant known from the late Early to the late Middle Miocene of Eurasia (*c*. 17.5–13.8 Ma). This new fossil material that includes several elements of the appendicular skeleton comes from the French sites of Pontlevoy (MN5), Aérotrain (MN4), and Artenay (MN4). The postcranial skeleton of *Amphimoschus* is relevant to determine its phylogenetic affinities within the Pecora and to better understand the evolution of cervoids, the pecoran ruminants more closely related to deer. Our total-evidence tip-dating phylogenetic analysis recovers three well-supported main lineages of crown pecorans (Giraffomorpha, Bovidomorpha and Cervidomorpha) and places *Amphimoschus* as a basal member of a monophyletic Cervoidea. Thus, we reject the recent assignment of *Amphimoschus* to the Bovoidea, and confirm the presence of hornless forms at the base of the cervoid clade. We define the Cervoidea as the least inclusive clade of crown pecorans including *Amphimoschus* and the Cervidae. We also define the Cervidomorpha as the least inclusive clade of crown pecorans containing *Namibiomeryx* and the Cervidae. Cervidomorphs were relatively successful in the Miocene, spreading through Africa, Eurasia and North America during the Early–Middle Miocene. *Amphimoschus xishuiensis* Y.-K. Li et al., 2021 is recovered here as the closest sister group to the Bovidae and hence cannot be considered to belong to the genus *Amphimoschus*. We erect for it the new genus *Dimidiomeryx*. Our topology adds complexity to the recently revamped hypothesis based on molecular data regarding the single origin of the cranial appendages in pecoran ruminants. *Amphimoschus* probably had a sitatunga-like lifestyle, sporting sprawling-out fingers with very long third phalanges, long limbs and a general configuration of the appendicular skeleton that probably allowed it to live in swampy/semiaquatic environments.

Keywords: body size; Cervoidea; headgear; Ruminantia; phylogeny; Miocene

Introduction

Amphimoschus Bourgeois, 1873 is an extinct hornless pecoran ruminant recorded from the late Early to the Middle Miocene of Eurasia (*c*. 17.5–13.8 Ma), a period of time mostly coincidental with the Miocene Climatic Optimum (Methner et al., 2020; Zachos et al., 2001). Its remains are mainly known from Central and Western Europe, mostly from France, Germany and Switzerland (see Mennecart et al., 2021 and references therein for a complete description and synthesis of all known European localities with *Amphimoschus*). As pointed out by Mennecart et al. (2021), these localities attest to diverse depositional environments such as swamps, lakes, rivers, karstic infillings and marine deposits. Fossils ascribed to *Amphimoschus* have also been cited from China (see e.g. C. K. Li et al., 1983; Y.-K. Li et al., 2021; Qui et al., 2013; Qiu & Qiu 2013; X.-M. Wang et al., 2013). Until recently, two species of *Amphimoschus* were classically recognized in Europe, *A. pontelevensis* Bourgeois, 1873 (type species; Thenay, Sables et Marnes du Blésois Formation, France) and the smaller and slightly older *A. artenensis* Mayet, 1908 (Artenay, Sables d'Orléanais Formation, France).

*Corresponding author. Email: micromeryx@gmail.com

Published online 18 Sep 2024

However, it has been recently argued that only *A. pontelevensis* should be considered valid for the European *Amphimoschus* due to the lack of a clear morphometric distinction among the cranial and dentognathic samples of the two species (Mennecart et al., 2021). A new Asian species, *A. xishuiensis* Y.-K. Li et al., 2021, has been recently described (Y.-K. Li et al., 2021). Yet since *A. xishuiensis* was merged with *Amphimoschus* in a single taxon prior to the phylogenetic analyses of Y.-K. Li et al. (2021), the status of this pecoran as a member of *Amphimoschus* is not fully resolved. *Amphimoschus* has relatively high-crowned lower molars that are distally closed, with the post-hypocristid contacting or almost contacting the post-entocristid (a parallelism with *Dremotherium*) but not fused to it as in bovidomorphs (Sánchez et al., 2010; Sánchez, Cantalapiedra, et al. 2015). It also has extended cristids/cristae, premolars with developed lingual structures, and several derived features of the inner ear (Mennecart et al., 2021, 2022).

Despite having a good European fossil record – including abundant dentognathic material and several complete skulls from which details as intricate as the inner ear morphology are known (Mennecart et al., 2021, 2022) – the phylogenetic affinities and systematics of *Amphimoschus* have been historically poorly comprehended, warranting the moniker 'enigmatic'. During the last 150 years almost all possible competing hypotheses of relationship of *Amphimoschus* within the Pecora have been proposed, with the exception of the Giraffomorpha. Bourgeois (1873) originally related *Amphimoschus* to the extant musk deer *Moschus* (hence the generic name) on the basis of its lack of cranial appendages, a hypothesis later revived by Rössner et al. (2013). Leinders (1983) linked *Amphimoschus* with the (in turn) enigmatic insular multi-horned pecoran *Hoplitomeryx*, a hypothesis followed by Janis and Scott (1987) and Mazza and Rustioni (2011), which included *Amphimoschus* in the Hoplitomerycidae. *Amphimoschus* was also closely allied with deer, as either a cervid or a cervoid (e.g. Mayet, 1908; McKenna & Bell, 1997; Roman & Viret, 1934; Rook et al., 1999; Stehlin, 1925) tying it together with the unstable historical definition and diagnosis of the Cervoidea (see Discussion section). Apart from being directly considered a 'Ruminantia indet.' (Kaiser & Rössner, 2007), Mennecart et al. (2021) recovered *Amphimoschus* as the sister group of the Antilocapridae (North American antelopes or pronghorns), but considered this genus a pecoran with uncertain phylogenetic affiliation. However, the currently most favoured hypothesis of relationship for this genus links *Amphimoschus* with the Bovoidea and/or the Bovidae (e.g. Bibi et al., 2009; Gentry, 1994, 2000; Gentry et al., 1999; Y.-K. Li et al., 2021; Mennecart et al., 2021; Mörs et al., 2000; Rössner, 1997, 2004; Solounias, 2007).

Amphimoschus was documented exclusively through dental and cranial remains, and its postcranial skeleton, to date, was almost totally unknown. The only published information regarding *Amphimoschus* postcranial material comes from its original description, in which Bourgeois (1873) figured a distal humerus and a metatarsal III–IV that he ascribed to *Amphimoschus*. This metatarsal III–IV lacks the distal end but shows a great part of the shaft, pertaining to a very slender-limbed pecoran. Unfortunately, Bourgeois (1873) did not describe the material in any detail, and not much information can be extracted from the figured illustrations. However, some postcranial material of *Amphimoschus* from the Loire Basin (France), consisting of appendicular elements of both fore and hind limbs, was excavated from 1962 onwards by the late Leonard Ginsburg (MNHN, Paris) (Ginsburg, 1990, and references therein). Due to various circumstances, these fossils remained unpublished until now, giving us the opportunity to describe them and partially fill the morphological data set of *Amphimoschus* with some postcranial data that can be used to test its purported bovoid affinities. The phylogenetic signal of the postcranial skeleton has been key in the past for establishing ruminant phylogenetic relationships, not only in pecorans but also in tragulids (e.g. Janis & Scott, 1987; Sánchez et al., 2010; Sánchez, Cantalapiedra, et al., 2015; Sánchez, Quiralte, et al., 2015). Additionally, the comparative morphofunctional study of this material could potentially give us hints about the lifestyle of *Amphimoschus* and the environment in which this pecoran lived.

The development of cranial appendages is one of the most notorious evolutionary novelties developed by pecoran ruminants and one of their most recognizable features. However, many pecorans were hornless and one extant family and a single deer species remain so (the Moschidae and the water Chinese deer, respectively), raising the question of the single (see e.g. Bubenik, 1990; Chen et al., 2019; Coope, 1968; Pilgrim, 1941, 1946; Y. Wang et al., 2019; Webb & Taylor, 1980) or multiple (see e.g. Gentry, 2000; Janis, 1982, 1986; Janis & Scott, 1987; Morales et al., 1993; Nieto et al., 2004) origin of pecoran headgear. The multiple-origin hypothesis predicts the existence of derived hornless lineages basal to the horned ones. The existence of these lineages was corroborated with e.g. the Moschidae, a derived clade of crown pecorans repeatedly recovered as the sister group of the horned Bovidae (see among others Guha et al., 2007; Hassanin & Douzery, 2003; Hassanin et al., 2012; Marcot, 2007;

Mennecart et al., 2021; Sánchez et al., 2010; Sánchez, Cantalapiedra, et al., 2015). Also, basal stem pecorans are hornless, there are multiple types of cranial appendages, and the distribution of the presence of headgear in the phylogenetic topologies containing fossil forms apparently favoured the multiple-origin hypothesis. However, recent molecular works including extant forms (Y. Wang et al., 2019) have challenged this hypothesis after the description of substantial similarities in the transcriptome profiling of different types of extant ruminant cranial appendages, consistent with a single origin in, at least, the ancestral crown pecoran, thus regarding moschids (and putatively all extinct hornless crown pecorans) as secondarily hornless, as in the living Chinese water deer *Hydropotes inermis* (Y. Wang et al., 2019). Hence, a conflict apparently exists between the output of molecular data sets composed exclusively by extant taxa vs morphological/total-evidence data sets that include fossils. It is, then, worth investigating whether (i) the phylogenetic position of *Amphimoschus* could shed some light on this subject and (ii) some other hornless pecoran lineages exist that constitute a similar case to moschids.

Hence, the aims of this work are: first, to describe in detail for the first time the available appendicular skeleton of *Amphimoschus*; second, to check the phylogenetic affinities of *Amphimoschus* within the Pecora using a total-evidence data set that includes postcranial data of *Amphimoschus* for the first time, contrasting the cervoid-bovoid competing hypotheses, and analysing as separate taxa the classic European *Amphimoschus* and the new Asian *A. xishuiensis*; and, third, to explore the palaeobiological and palaeoecological implications that can be drawn from the appendicular anatomy of *Amphimoschus*, including a body size evaluation based on the postcranial skeleton.

Material and methods

Material

The postcranial material of *Amphimoschus* described in this work was part of the collection curated by the late Leonard Ginsburg (MNHN, Paris, France) and comes from three sites of the Loire Basin (France; Fig. 1): Artenay (MN4), Aérotrain (MN4) and Pontlevoy (MN5). The osteological and fossil materials used for the phylogenetic analyses are the same as those reported in Sánchez, Cantalapiedra, et al. (2015). We have used two *Tragelaphus spekii* specimens (collection numbers 143 and 1016) from the Museo Anatómico de la Universidad de Valladolid (Valladolid, Spain) for the comparative morphofunctional study of *Amphimoschus*.

Fig. 1. Geographical location of the three French fossil sites (Pontlevoy, Artenay and Aérotrain) that produced the *Amphimoschus* postcranial skeleton described herein.

All the material of *Amphimoschus* presented in this work is curated by the Musèum national d'Histoire naturelle in Paris, France (MNHN). The mitochondrial genomes of *Hyemoschus*, *Muntiacus*, *Capreolus*, *Moschus*, *Eudorcas*, *Giraffa* and *Antilocapra* are part of the original data set presented by Hassanin et al. (2012) and were downloaded from GenBank (accession numbers available in Hassanin et al., 2012).

Phylogenetic analysis

We performed a set of total-evidence Bayesian tip-dating phylogenetic analyses to explore the relationships of *Amphimoschus* within the Pecora. We used the original data sets of Sánchez, Cantalapiedra, et al. (2015), both morphological and molecular, with the addition of *Amphimoschus pontelevensis* (i.e. European *Amphimoschus*) and '*A*'. *xishuiensis*, for a total of 29 terminals. The scoring of the characters of '*Amphimoschus*' *xishuiensis* was carried out after the thorough examination of the published images of this taxon in Y.-K. Li et al. (2021). The matrices are presented as Supplemental material.

The morphological data matrix has 67 characters (with character 9 removed as it has no variation among this sample), was compiled in MacClade v. 4.05 and was transformed using Mesquite v. 3.01 (Macintosh versions). Likelihood-based phylogenetic inference has been acknowledged to be less sensitive to homoplasy than traditional parsimony, which treats fast-evolving (homoplasic) and conservative characters in the same way (Lee & Worthy, 2012). The 'tip-dating' method provides a simultaneous estimation of tree topology and divergence times based on a relaxed morphological and/or molecular clock and the temporal uncertainty of the first stratigraphic record of each species (Grimm et al., 2015; Ronquist et al., 2012). The morphological data set

was complemented with molecular sequences for four mitochondrial genes (12S, 16S, CytB and COX3). We used these genes because their inclusion in previous studies (Sánchez, Cantalapiedra, et al., 2015) allowed for a better assessment of the impact of adding new fossil taxa to the data set. The mitochondrial sequences were gathered for the seven extant genera (*Hyemoschus*, *Muntiacus*, *Capreolus*, *Moschus*, *Eudorcas*, *Giraffa* and *Antilocapra*) included in the morphological matrix. We ran our total-evidence analyses in a Bayesian framework using BEAST v. 2.6.7 (Bouckaert et al., 2014). The input xml file was prepared in the software BEAUTi. We recorded variable characters only and used the same clock model for all the data sets. We used a Lewis model with four gamma categories for the morphological characters, and a GTR model with four gamma categories and the proportion of invariant sites set to zero for the molecular sequences. An uncorrelated lognormal relaxed molecular clock model was implemented.

We used default priors for all the parameters. Then we set a monophyly constraint that forced the basalmost divergence between *Hyemoschus* and the Pecora. These settings correspond with our free total-evidence analysis (Tree 1). We then ran a version of the analysis that incorporated a temporal prior at the node containing all crown Pecora (excluding *Hyemoschus*, *Gelocus* and *Amphitragulus*; Tree 2), with a prior being gamma distribution with parameters alpha = 2, beta = 0.5 and offset 20.44. This prior provides a hard lower limit for the split at the end of the earliest Miocene (Aquitanian), and a soft upper limit with the 97.5% quantile at 23.2 Ma, aiming to keep the divergence age within the Early Miocene. To test the impact of the DNA-derived hypothesis that both giraffids–antilocaprids and bovids–cervids are sister taxa (Chen et al., 2019; Y. Wang et al., 2019), we built a third model (Tree 3) where the clades Antilocaproidea (Antilocapridae + Merycodontidae) and Giraffomorpha (Palaeomerycoidea + Giraffoidea), and Bovoidea and Cervoidea were forced to form monophyletic lineages. We used the fossilized birth–death (FBD) model and set the removal probability to 1 to obtain fully bifurcating trees.

We ran four Markov chain Monte Carlo (MCMC) chains for 100 million generations each, sampling every 1000 generations. After inspection in Tracer (Rambaut & Drummond 2016), we used LogCombiner and TreeAnnotator (available at http://beast.bio.ed.ac.uk/programs) to discard 20% of each chain as burn-in, to resample the posterior to obtain a combined tree distribution of 10,000 trees, and to produce maximum credibility trees. The robustness of phylogenetic affinities was assessed based on the posterior probability (pp) of branches.

Body size estimates

We predicted body mass (in kg) in *A. ponteleviensis* (*sensu* Mennecart et al., 2021) as a measurement of body size using teeth and humeri (Table 1). We choose to work with these variables because the correlation between them and body size in a wide variety of living ruminants has been successfully tested (Janis, 1990b; Scott, 1990) allowing accurate estimates of body mass for extinct species (DeMiguel, 2016; DeMiguel et al., 2012; Janis, 1990a; Sánchez et al., 2022). We calculated results from two independent (i.e. craniodental and limb) sources to check for differences in the results and to estimate whether our fossils give a signal of macrodonty. We calculated the mean body mass for each specimen following regression equations by Janis (1990b) and Scott (1990) for (occlusal) length measurements of their molars and the transverse width of the distal articulation of the humerus, respectively, and then for each site by averaging the mean across individuals (Table 1). Regarding teeth, only lower molars and maxillary second molars were evaluated. When several specimens (i.e. different tooth positions) from the same individual were available, only the first molar was selected for analysis. Only adult specimens (i.e. complete molar growth and fused distal humeral epiphyses) were considered for analyses.

Measurements

All measurements were taken with digital callipers and are presented as Supplemental material. We follow the

Table 1. Summary of body mass (in kg) estimates for *Amphimoschus*. Body mass comparison in *Amphimoschus* inferred from cranial (molar length) and postcranial (transversal width of the distal articulation of the humerus) variables. **Abbreviations: Avg**, average; **lM**, (occlusal) length measure of the molars; **m1**, first lower molar; **m2**, second lower molar; **m3**, third lower molar; **M2**, second upper molar; **N**, number of specimens measured; and **tdH**, transverse diameter of the humerus.

Species	Site	N	m1	m2	m3	M2	Avg lM	N	Avg tdH
A. pontelevensis	Pontlevoy	4	38.7/N = 2	51.7/N = 1	–	49.9/N = 1	46.7	2	36.71
A. pontelevensis?	Artenay	49	40.4/N = 16	36.2/N = 13	52.5/N = 10	36.7/N = 10	42.1	2	36.01

set of postcranial measurements proposed by Sánchez and Morales (2008).

Institutional abbreviation

MNHN, Musèum national d'Histoire naturelle (Paris, France).

Other abbreviation

CDA, common digital artery.

Systematic palaeontology

Mammalia Linnaeus, 1758
Cetartiodactyla Montgelard, Catzeflis and Douzery, 1997
Ruminantia Scopoli, 1777
Pecora *sensu* Webb and Taylor, 1980
Cervidomorpha new clade

Diagnosis. Crown pecorans with lacrimal fossa located in front of the lacrimal orifice(s); parieto-squamosal suture in the middle of the temporal fossa; and p4 with mesolingual conid joining the cristid obliqua through the postero-lingual cristid.

Cervoidea Simpson, 1931

Definition. The least inclusive clade of crown-pecorans containing *Namibiomeryx* and the Cervidae.

Emended diagnosis. Crown pecorans with two lacrimal orifices, one of them clearly above the other; ethmoidal vacuity interrupting nasal/lacrimal contact; slit-like elliptical opening in the border of the mastoid; canal of the digital common artery (CDA) of 'cervid type' (*sensu* Sánchez *et al.* 2010); well-developed plantar metatarsal tuberosity; and smooth and sloped lateral border of the dorsodistal process of the tibia.

Amphimoschus Bourgeois, 1873
(Figs. 2–4)

Type species. *Amphimoschus ponteleviensis* Bourgeois, 1873.

Emended diagnosis. Anteroposteriorly wide retro-articular process with well-developed posterior expansions; lacrimal fossa absent; foramen ovale and infratemporal fossa separated by a well-developed crest; post-entocristid almost contacting the post-hypocristid; bicuspidate third lobe of the m3, with presence of well-developed post-entoconulidcristid; double facet for the entocuneiform in the metatarsal III–IV; plantar portion of the proximal metatarsal articular surface clearly differentiated from the dorsal portion by lateral and medial incisures; presence of two facets for the entocuneiform in the metatarsal III–IV separated by a distinct groove; elongated, sitatunga-like third phalanges; quadrangular and relatively high navicular-cuboid, with straight (non-rounded) dorsal, lateral and medial borders; well-developed humeral epicondylar crest, pointing dorsally with sharp lateral border. Also, after Mennecart et al. (2021): diastema between the upper/lower canine and the upper/lower cheek teeth is almost equal to the anterodistal length of P/p2–4; maxillary with a strong facial crest at orbit level; auditory bullae with elongated neck and posterior styloid process; bony labyrinth with elongated cochlea detached from the vestibule, and relatively similar thickness of the different coils; petrosal bone with large epitympanic wing that encircles the promontorium, blunt apex, large and round fossa for the tensor tympani muscle, and presence of a dorsal basicapsular groove.

Material. Pontlevoy: MNHN.F. FP 2565 (right navicular-cuboid), MNHN.F. FP 2582 (proximal fragment of left metatarsal III–IV); Artenay: MNHN.F. Ar 5774 (distal fragment of right humerus), MNHN.F. Ar 4706 (right metacarpal III–IV), MNHN.F. Ar 6178 (right metatarsal III–IV), MNHN.F. Ar 4548 (right astragalus); MNHN.F. Ar 4610 (right navicular-cuboid), MNHN.F. Ar 5325 (first phalanx), MNHN.F. Ar 5324 (second phalanx), MNHN.F. Ar 5389 (third phalanx). Aérotrain: MNHN.F. Or 601 (left radius).

Description

Humerus (Fig. 2I–J). The single available specimen (MNHN.F. Ar 5809) corresponds to a distal humeral fragment. The proximal and distal borders of the trochlea are convergent, non-parallel. The capitulum is well developed, especially distally, reaching the level of the distal border of the trochlea. In this regard it is very similar to *Moschus*. However, the keel rising between the capitulum and the trochlea is more developed in *Amphimoschus* than in the extant musk-deer. The coronoid fossa is triangular and well marked. The epicondilar crest points dorsally and is well developed, with a sharp lateral border. This structure is much more developed than in the bovid *Eotragus* or Middle Miocene deer such as *Dicrocerus* or *Heteroprox*.

Radius (Fig. 2C–D). The radius is slender, *Moschus*-like. The trochlear-capitular articular complex is dorso-palmarly wide, giving a rectangular profile to the proximal articular surface. In this respect it is also similar to *Moschus*. The extant musk-deer has a capitular facet that is relatively wider and more dorsally developed, however. The palmar notch between the capitular and trochlear facets is relatively deep, more than in *Moschus*. The two facets for the ulna are separated. Disto-dorsally, the sulcus for the radial extensor tendon

Fig. 2. *Amphimoschus ponteleviensis*, long bones. **A**, MNHN.F. Ar 4706, right metacarpal III–IV in dorsal view; **B**, MNHN.F. Ar 4706, right metacarpal III–IV in palmar view; **C**, MNHN.F. Or 601, left radius in dorsal view; **D**, MNHN.F. Or 601, left radius in palmar view; **E**, MNHN.F. Ar 6178, right metatarsal III–IV in dorsal view; **F**, MNHN.F. Ar 6178, right metatarsal III–IV in plantar view; **G**, MNHN.F. FP 2582, proximal fragment of left metatarsal III–IV in dorsal view; **H**, MNHN.F. FP 2582, proximal fragment of left metatarsal III–IV in plantar view; **I**, MNHN.F. Ar 5774, distal fragment of right humerus in dorsal view; **J**, MNHN.F. Ar 5774, distal fragment of right humerus in palmar view. **Abbreviations**: **EpC**, epicondilar condyle; **PMtTub**, plantar metatarsal tuberosity; **SaF**, supraarticular fossae; **TbCol**, tubercles for the collateral ligaments.

of the carpus is wide and well marked, with two sharp parallel crests delimiting its borders. Palmarly, the attachment marks for the ulnar ligaments are strong. The facet for the semilunar has a lateral notch, as occurs e.g. in *Hispanomeryx*.

Metacarpal III–IV (Fig. 2A–B). The metapodials of *Amphimoschus* are also characteristic of a slender-limbed animal. Probably corresponding to a single individual, metapodials from Artenay show that the metacarpal III–IV of *Amphimoschus* was only slightly shorter than the metatarsal III–IV (with under 2 cm of difference, they can be considered sub-equal in length). The proximal articular surface of the metacarpal III–IV is semicircular, with the facet for the magnotrapezoid taking up more than half of the proximal articular surface. There is a deep non-articular notch between the two proximal articular surfaces. The sulcus for the lateral extensor tendon is proximally deep, and well marked all along the bone length. There is a very thin but well-marked dorsal sulcus that is distally closed 1 cm above the distal articulation trochleae. The supraarticular fossae are far less marked than in *Moschus*; this is also the case for the articular keels. The insertion tubercles for the collateral ligaments are also less developed than in the extant musk-deer. The intertrochlear incision is 'U'-shaped.

Astragalus (Fig. 3A–B). The astragalus is slender, similar to that of *Moschus*. The latero-proximal condyle is higher than the medial one. The plantar trochlea is very well developed, contacting distally the medial condyle of the distal trochlea. In dorsal view, the lateral border of the distal trochlea is inclined but does not develop a notch as in e.g. some *Micromeryx*.

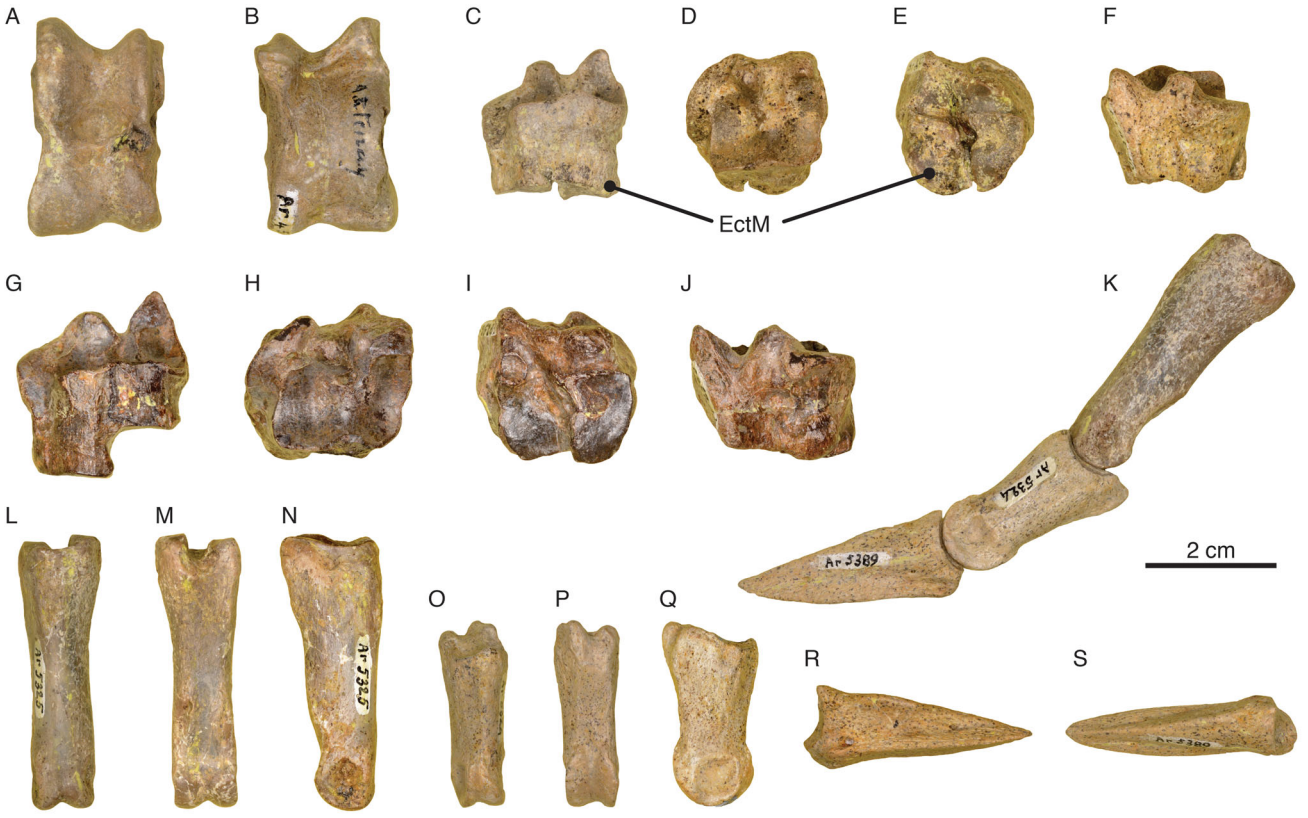

Fig. 3. *Amphimoschus ponteleviensis*, tarsal bones and phalanges. **A**, MNHN.F. Ar 4548, right astragalus in dorsal view; **B**, MNHN.F. Ar 4548, right astragalus in plantar view; **C**, MNHN.F. Ar 4610, right navicular-cuboid in dorsal view; **D**, MNHN.F. Ar 4610, right navicular-cuboid in proximal view; **E**, MNHN.F. Ar 4610, right navicular-cuboid in distal view; **F**, MNHN.F. Ar 4610, right navicular-cuboid in plantar view; **G**, MNHN.F. FP 2565, right navicular-cuboid in dorsal view; **H**, MNHN.F. FP 2565, right navicular-cuboid in proximal view; **I**, MNHN.F. FP 2565, right navicular-cuboid in distal view; **J**, MNHN.F. FP 2565, right navicular-cuboid in plantar view; **K**, composite digit in external view (MNHN.F. Ar 5325, MNHN.F. Ar 5324, MNHN.F. Ar 5389); **L**, MNHN.F. Ar 5325, first phalanx in dorsal view; **M**, MNHN.F. Ar 5325, first phalanx in posterior view; **N**, MNHN.F. Ar 5325, first phalanx in interdigital view; **O**, MNHN.F. Ar 5324, second phalanx in dorsal view; **P**, MNHN.F. Ar 5324, second phalanx in posterior view; **Q**, MNHN.F. Ar 5324, second phalanx in interdigital view; **R**, MNHN.F. Ar5389, third phalanx in interdigital view; **S**, MNHN.F. Ar5389, third phalanx in dorsal view. **Abbreviation**: **EctM**, ectomesocuneiform.

Navicular-cuboid (Fig. 3C–J). The navicular-cuboid of *Amphimoschus* is tall, clearly taller than that of *Eotragus* and Miocene deer. The proximal articulation surface is markedly square, with the dorsal, lateral and medial borders clearly straight, very different from the rounded proximal articular surface of the navicular-cuboid of *Eotragus*, *Heteroprox* or *Procervulus*. The lateral facet for the astragalus is much wider than the medial. The plantomedial process is high and pointed, as occurs in *Micromeryx*. The facet for the calcaneum is very inclined, almost vertical at its distal end. The rounded notch lateral to the plantomedial process is well marked. This process is relatively short, similar to that of the moschid *Hispanomeryx*. There is a marked 'Y'-like structure in the lateral part of the plantar surface. The distal part of that Y develops a weak round crest apparently less developed than the same structure present in cervids. However, MNHN.F. Ar 4610 is eroded and the real development of the plantar structures may be distorted. Lateral to that crest there is a flattish surface that does not form a canal. The dorsal metatarsal facet is sub-triangular with a lateral notch. The plantar metatarsal facet, separated from the dorsal one by a groove, is elongated and inclined centro-medially, rising to the central part of the bone. The ectomesocuneiform is fused to the navicular-cuboid in the Artenay specimen. Whether this feature is autapomorphic for a second species of *Amphimoschus* different from *A. ponteleviensis* (i.e. *A. artenensis*) or a characteristic of this particular navicular-cuboid (e.g. a fusion due to either age or a previous pathology) cannot be known due to the lack of additional specimens. The

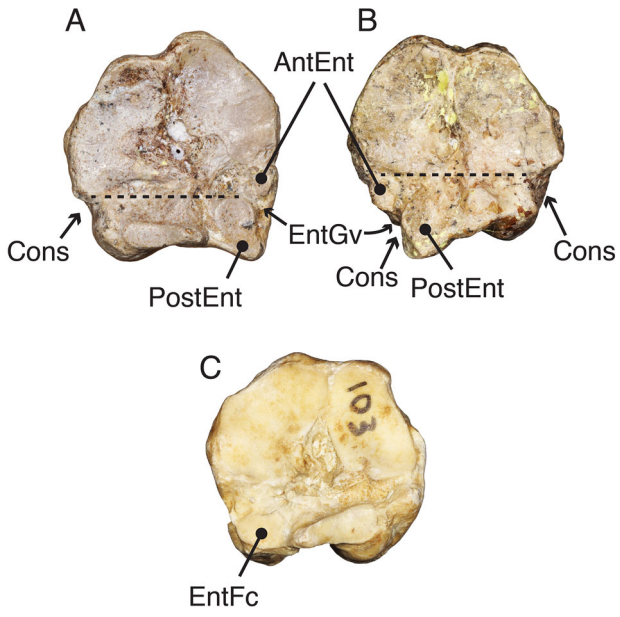

Fig. 4. Comparative morphology of the proximal surface of the metatarsal III–IV of *Amphimoschus ponteleviensis*. **A**, MNHN.F. FP 2582, left metatarsal III–IV, Pontlevoy (France); **B**, MNHN.F. Ar 6178, right metatarsal III–IV, Artenay (France); **C**, *Heteroprox* (Cervidae), MNHN.F. Sa 8960, right metatarsal III–IV, Sansan (France). The dotted line marks the plantar portion of the proximal metatarsal articular surface, clearly differentiated from the dorsal portion by lateral and medial constrictions. The pictures are not shown to scale, for comparative purposes. **Abbreviations**: **AntEnt**, anterior entocuneiform facet; **Cons**, constriction; **EntFc**, entocuneiform facet; **EntGv**, groove between the anterior and posterior entocuneiform facets; **PostEnt**, posterior entocuneiform facet.

facet for the entocuneiform is large, sub-rectangular and flat.

Metatarsal III–IV (Fig. 2E–F). MNHN.F. FP 2582 (Pontlevoy) is substantially larger than MNHN.F. Ar 6178 (Artenay). The proximal surface is pentagonal, with a medially located column that bears the facet for the entocuneiform, similar to that of *Micromeryx* and *Moschus*. The dorsal facet for the navicular-cuboid is sub-triangular to sub-elliptical, comparatively shorter than its *Moschus* homologue. In MNHN.F. FP 2582 there is a central non-articular synovial groove. The plantar facet for the navicular-cuboid is fusiform in MNHN.F. FP 2582 and shorter and rounded in MNHN.F. Ar 6178, and has a elevated medial tip, forming a triangular point in the plantar border of the proximal articular surface. The kidney-shaped facet for the ecomesocuneiform is more dorsally projected than the dorsal facet for the navicular-cuboid, and is the largest of the proximal set of articular facets. There are two facets for the entocuneiform (Fig. 4), including a larger plantar one, sub-quadrangular and flat (more elongated in MNHN.F. FP 2582 than in MNHN.F. Ar 6178), and a dorsal smaller sub-circular facet located between the facet for the ectomesocuneiform and the main facet for the entocuneiform. Both entocuneiform facets are distinctly isolated from each other and separated by a groove. In some pecorans (e.g. *Heteroprox*) the anterior (dorsal) part of the entocuneiform facet is smaller and distinct but remains connected to the main facet, never split in two (Fig. 4C). The double facet thus appears to be a good diagnostic feature of *Amphimoschus* metatarsals. The plantar surface that contains both plantoproximal facets is clearly separated from the main proximal articular surface. This separation is marked by lateral and medial incisures very easily observed in proximal view. These lateral and medial notches are well marked in the form from Artenay, whereas the lateral one is more marked than the medial in the younger *Amphimoschus* from Pontlevoy (MNHN.F. FP 2582). However, the separation of the plantoproximal facets in a surface/platform of their own is nevertheless obvious also in MNHN.F. FP 2582. The furrow for the lateral extensor tendon is proximally very similar in both MNHN.F. FP 2582 and MNHN.F. Ar 6178, relatively long and proximally less marked than in *Moschus*. Only MNHN.F. Ar 6178 is complete, including the distal part and the entire diaphysis. The dorsal metatarsal sulcus is well marked and distally closed. The canal for the CDA is of 'cervid-type' (Sánchez et al., 2010). It is very easy to check this condition since the medial distal trochlea is missing and the bone is broken, exposing said canal. As occurred with the metacarpal III–IV, the insertion tubercles for the collateral ligaments are less marked than in *Moschus*, and also the supraarticular fossae are less developed.

First phalanx (Fig. 3K–N). The central sulcus of the proximal articulation surface is dorsally closed. The external facet of this surface is dorsally triangular, similar to that of *Moschus* but more elongated. The furrow for the tendon of the interosseus muscle is relatively long but poorly marked. The insertion area for the interdigital ligament is elongated and elliptical but also poorly marked. The insertion areas for the sesamoid ligaments are well marked and are more vertically developed than in *Moschus*. The dorsal surface is slightly concave and the palmar surface is almost straight with the palmar concavity starting at the beginning of the distal third of the phalanx. In interdigital view the distal facet expresses a distinct palmar angle.

Second phalanx (Fig. 3K, O–Q). In proximal view, the proximal articulation surface is relatively narrow and triangular. The external articular facet is slightly longer than the interdigital one. By comparison, moschids have

a wider proximal articulation area. The post-articular plateau is well developed and proximally pointed. The extensor process is short. The insertion area for the flexor digitorum superficialis tendon is well marked. In interdigital view, the distal facet is distally 'angled' as in cervids (Köhler, 1993) and *Moschus*.

Third phalanx (Fig. 3K, R–S). The third phalanx is extraordinarily elongated with an expanded and concave palmar surface. The extensor process is very small. Similar to *Moschus*, the proximal surface is almost completely occupied by the articular area, with a very small platform for the flexor digitorum profundus tendon.

Bovidomorpha Sánchez, Cantalapiedra, Ríos, Quiralte, and Morales, 2015

Emended diagnosis. Crown pecorans with laterally inflated tympanic bulla with well-developed posterior expansion; postglenoid foramen laterally closed due to the expansion of the tympanic bulla; contact between the acoustic tube and the mastoid bone; completely or almost completely aligned lingual cuspids in the lower molars; absent upper canines in males; highly developed post-entocristid that completely fuses with the post-hypocristid, distally closing the lower molars; more or less flattened lower molar cuspids, with narrow lingual ribs; elongated and wide capitular facet in the radius; distally open metatarsal sulcus; developed proximo-plantomedial process of the navicular-cuboid; proximo-plantomedial process of the navicular-cuboid without any crest; navicular-cuboid without canal in the plantar side of the bone, lateral to the proximo-plantomedial process.

Bovoidea Gray, 1821 *sensu* Sánchez, Domingo, and Morales, 2010

Genus ***Dimidiomeryx*** gen. nov.

Diagnosis. As for the type and only species.

Type and only species. *Dimidiomeryx xishuiensis* (Y.-K. Li, Mennecart, Aiglstorfer, Ni, Li & Deng, 2021)

Derivation of name. Latin (*Dimidium*) for 'half' and Greek (*Meryx*) for 'ruminant', meaning 'the ruminant in the middle' in reference to its phylogenetic position between moschids and bovids within the Bovoidea.

Dimidiomeryx xishuiensis (Y.-K. Li, Mennecart, Aiglstorfer, Ni, Li, & Deng, 2021)

2003 *Amphimoschus* cf. *A. artenensis* X.-M. Wang et al.: 262.
2008 *Amphimoschus* cf. *A. artenensis* X.-M. Wang et al.: 3, fig. 8.
2021 *Amphimoschus xishuiensis* Y.-K. Li et al.: 3, figs. 2–3.

Emended diagnosis. Headgear composed of four small bumps, two supraorbital and two anteorbital; bicuspidate third lobe of the m3 with small or very small entoconulid. Also, after Y.-K. Li et al. (2021): narrow p4 with broad cristid obliqua; well-developed metastylids in the lower molars; presence of additional stylid at the lingual base of the lower molars; and presence of anterolingual cingulum in the P4.

Material. The original material was described in Y.-K. Li et al. (2021).

Occurrence and age. After Y.-K. Li et al. (2021): Xishuigou, East gully of the Tabenbuluk area, Subei Mongolian Autonomous County, Gansu Province, China. Xishuigou Fauna (X.-M. Wang et al., 2008), Tiejianggou Formation, *c*. 19.7–17 Ma, late Early Miocene (X.-M. Wang et al., 2013).

Results

Body mass estimates

Molar length estimates of body mass in *Amphimoschus ponteleviensis* range from 42 kg in Artenay to 47 kg in Pontlevoy (Table 1). Humeral estimates provide a body mass of approximately 36 kg in both *A. ponteleviensis* from Pontlevoy and Artenay (Table 1). Thus, calculated body size values of *Amphimoschus* were higher from dentition-based estimates (17% Artenay–27% Pontlevoy/Thenay) than from postcranial measures (Table 1). This difference probably reflects the presence of a certain degree of macrodonty in *Amphimoschus*.

Phylogenetic analysis

All recovered trees (Fig. 5) show three well-supported main clades of crown pecorans (giraffomorphs, bovidomorphs, and the taxa more related to cervids or cervidomorphs), including a very robust Cervoidea (Tree 1, pp = 0.98; Tree 2, pp = 0.97; Tree 3, pp = 0.89) including *Amphimoschus* as its basal offshoot. '*Amphimoschus*' *xishuensis* Y.-K. Li et al., 2021 does not cluster with *Amphimoschus* and instead is always recovered as the sister group of the Bovidae (Tree 1, pp = 0.63; Tree 2, pp = 0.53; Tree 3, pp = 0.51) within a monophyletic Bovoidea (Tree 1, pp = 0.75; Tree 2, pp = 0.68; Tree 3, pp = 0.80) also including the Moschidae. The reconstructed morphological apomorphies of *Amphimoschus* and the discussed clades for our working Tree 2 are presented in Table 2.

Discussion

According to our phylogenetic analyses, *Amphimoschus* is a hornless basal member of a monophyletic Cervoidea

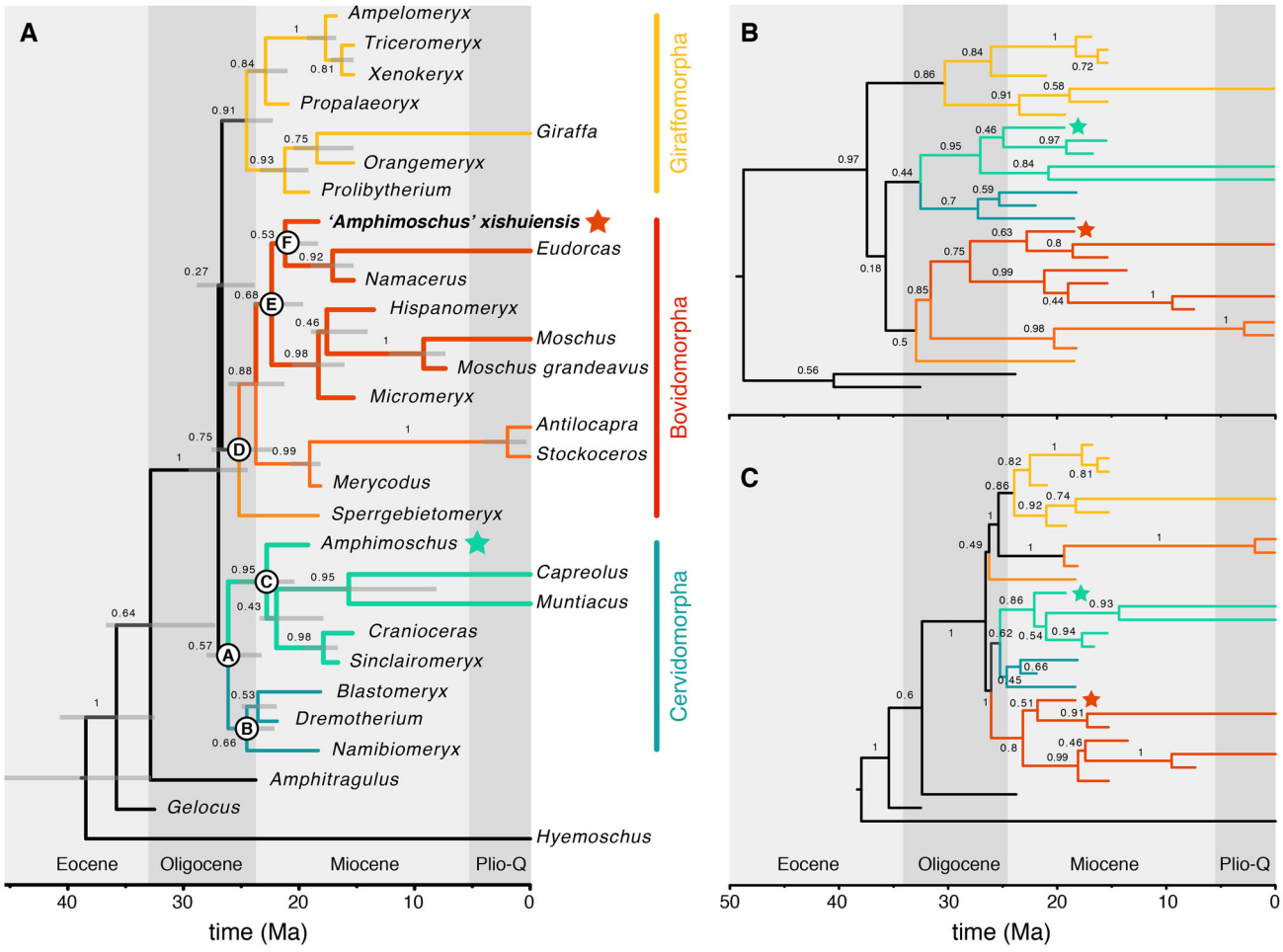

Fig. 5. Maximum clade credibility time-trees of major pecoran clades obtained by tip-dating Bayesian analysis. Numbers next to each node represent the posterior probability (pp) of each respective clade. In each tree the green star marks *Amphimoschus* and the red star marks *Dimidiomeryx xishuiensis* ('*Amphimoschus*' *xishuiensis* in the tree). **A**, Tree 2 (temporal prior on crown Pecora). Uncertainty in divergence ages is shown with horizontal bars representing their 95% higher posterior densities (HPDs); **B**, Tree 1 (free, no temporal prior). This tree recovers a sister-group relationship between bovidomorphs and cervidomorphs as in Chen et al. (2019); however, the very low posterior probability at the base of this node indicates that this analysis and data set cannot resolve the basal polytomy among the three main crown-pecoran lineages (Bovidomorpha, Giraffomorpha and Cervidomorpha). The *Hyemoschus* line has been removed from Figure 7B for visualization purposes; **C**, Tree 3 (temporal prior on crown Pecora and forced Antilocaproidea + Giraffomorpha and Bovidomorpha + Cervidomorpha). **Nodes**: A, Cervidomorpha; B, unnamed clade (non-cervoid cervidomorphs); C, Cervoidea; D, Bovidomorpha; E, Bovoidea; F, unnamed clade (*Dimidiomeryx xishuiensis* + Bovidae).

Table 2. Reconstructed morphological character/states for the discussed internal nodes of Bayesian Tree 2, the topology of which is discussed in the text. Ambiguous synapomorphies in italics.

Node/taxon	Character (state)
Node A (Cervidomorpha)	*16(1)*; 20(0); *63(1)*
Node B (Cervoidea)	7(1); 18(2); 54(2); 57(1); *65(1)*
Node C (Unnamed clade)	*2(2)*; *3(1)*; 36(1); *65(0)*
Node D (Bovidomorpha)	12(2); *16(0)*; 24(1); 39(1); 41(2); *49(1)*; *51(1)*; *59(0)*; *62(1)*; *63(0)*; *64(0)*
Node E (Bovoidea)	2(1); 10(2); *40(2)*; 42(1); *51(1)*; *62(1)*
Node F (Unnamed clade)	15(0); 16(1); *20(0)*; *23(1)*; *53(1)*; *55(0)*
Amphimoschus	10(2); *16(0)*; 23(1); 39(1); 41(1); 44(1); 51(0)
Dimidiomeryx xishuiensis	14(8); 45(2)

(Fig. 5). Notably, this outcome remains valid across the three analyses with different topological and temporal constraints. Both the definition and diagnosis of the Cervoidea have varied enormously through the years. Stirton (1944) and Romer (1966) considered the Giraffidae, the Moschidae and the Cervidae as cervoids. Hamilton (1978) linked the Cervidae to the Moschidae into the Cervoidea. Leinders and Heintz (1980) included moschids, antilocaprids and cervids within the Cervoidea, and united these families by the presence of a double lacrimal orifice in the orbit rim and distally closed metatarsal gully in the metatarsal III–IV. Leinders (1983) considered that the Cervoidea was diagnosed by the presence of a distally closed metatarsal gully, and linked together moschids, antilocaprids, hoplitomerycids, dromomerycids and cervids as cervoids. Geraads et al. (1987) and Gentry and Hooker (1988) defined the Cervoidea as containing the Palaeomerycidae – including dromomerycids – the Cervidae, *Dremotherium*, *Moschus* and *Hydropotes*. Janis and Scott (1987) and Scott and Janis (1987) thoroughly discussed the ingroup pecoran relationships and the diagnosis and definition of cervoids, diagnosing them by the presence of: 'traguloid' enlarged upper canine; *Palaeomeryx*-fold in the lower molars; completely fused metapodials with distally closed metatarsal gully; and slightly raised cubonavicular facet in the metatarsal III–IV. They included in the Cervoidea many pecoran taxa: *Eumeryx*, *Rutitherium*, *Walangania*, the 'Moschidae' (including *Dremotherium* and blastomerycids), the Antilocapridae (including merycodontids or merycodontines), the Palaeomerycidae (including dromomerycids, *Amphitragulus* and *Prolybitherium*), the Hoplitomerycidae (including *Amphimoschus*), and the Cervidae, with the antlerless Chinese water deer *Hydropotes* as the sister group of all antlered cervids. Finally, Gentry (2000) defined a Cervoidea comprising moschids (including blastomerycines), palaeomerycids (including dromomerycids), cervids, antilocaprids, *Hoplitomeryx* and *Walangania*. Here we define the Cervoidea as the least inclusive clade of crown pecorans containing *Amphimoschus* and the Cervidae. We diagnose the Cervoidea on the basis of a suite of reconstructed morphological synapomorphies (Table 2) that links *Amphimoschus* to cervids and dromomerycids. This suite comprises both cranial and postcranial features: presence of two lacrimal orifices (one of them clearly above the other); slit-like elliptical opening in the border of the mastoid; canal of the CDA of 'cervid type' (Sánchez et al., 2010); and well-developed plantar metatarsal tuberosity – a parallelism of cervoids and moschids (see also Sánchez et al., 2010). Some of these traits (e.g. the double lacrimal orifices, and the developed ethmoidal vacuity cutting the nasal/lacrimal contact; Janis & Scott, 1987) have been considered cervid synapomorphies in the past. Our reconstructed character/state distribution clearly rejects as diagnostic of cervoids the distally closed metatarsal gully, the most classically proposed cervoid diagnostic feature (see among others Gentry et al., 1999; Janis & Scott, 1987; Prothero, 2007). As discussed in Sánchez et al. (2010) the open/closed status of the distal part of the dorsal metatarsal gully is directly related to the disposition of the canal of the CDA, which can be extremely superficial (bovid-type), superficial (moschid-type) or deep, running very close to the bone axis (cervid-type). It was hypothesized (Sánchez et al., 2010) that, when a moschid-type CDA is present – in fact the most widespread state of this character among pecorans – both open and closed sulci can be present in a single lineage. This prediction was corroborated in the Moschidae, with two lineages presenting a closed sulcus (*Micromeryx* and *Moschus*) and another one (*Hispanomeryx*) having an open state of the character (Sánchez et al., 2010). Only when the CDA is of cervid-type, very deep, as in the case of cervoids – and also antilocaprids outside the Cervoidea – is the sulcus fixed in the closed state. In our topologies, the closed metatarsal sulcus is recovered as ambiguously primitive for the clade *Amphitragulus* + crown Pecora. Also, Janis and Scott (1987) postulated that cervoids sport 'traguloid' enlarged upper canines in males. However, cervoids such as *Amphimoschus* have moschid-type (Sánchez et al., 2010) enlarged upper canines. The cervid-type morphology as described in Sánchez et al. (2010) – the same as the 'traguloid' condition of Janis and Scott (1987) – is restricted to the Cervidae within the Pecora. The only exception among cervids is the Chinese water deer *Hydropotes*, which is not only secondarily antlerless but also secondarily 'fanged'. *Hydropotes* shows the basal pecoran condition of enlarged moschid-type canines present in stem pecorans, non-cervid cervidomorphs, palaeomerycoid giraffomorphs and moschid bovidomorphs (Sánchez, Cantalapiedra, et al., 2015), thus regaining not the ancestral cervid state, but the ancestral pecoran state. The double lacrimal orifice in the orbit rim is also a classic cervoid character that needs some refining, since cervoids are characterized by having two lacrimal orifices that are very clearly one above the other. The cases of *Amphimoschus* as a hornless cervoid and musk deer as hornless bovoids demonstrate that, when using a sufficiently wide and diverse data set (including if possible cranial, dental and postcranial subsets), the phylogenetic affinities of hornless ruminants are not intrinsically more difficult to unveil than those of the horned groups due to the lack of cranial appendages, despite arguments to the contrary (Mennecart et al., 2021).

Recently, several authors (Y.-K. Li et al., 2021; Mennecart et al., 2021) have raised the hypothesis of the putative 'horned' condition of European *Amphimoschus*, basing their arguments on the presence of a thickened/enlarged ante-supraorbital area in the *Amphimoschus* partial skull PIMUZ A/V4656 from Wildenbusch and Benken (Switzerland; see Mennecart, 2021 for recent pictures of this material). Mennecart et al. (2021) related these ante-supraorbital bony ridges with the strong facial ridges of the extant muntiacine deer *Muntiacus*, in which the long pedicles extend rostrally to result in strong facial ridges, implying that the presence of the facial ridges is a way to infer the existence of cranial gear in pecorans even if the actual appendages are not preserved in the fossil. Some cervids show post-supraorbital bony ridges connecting the pedicles with the orbits that have also been related to the facial ridges of muntjacs, considering this a primitive trait, as muntiacines are generally regarded as the most primitive among extant antlered deer. Contrary to this interpretation, *Muntiacus* facial ridges can be considered an autapomorphic character (Croitor, 2014). They are present in both genders as adults and even exist in yearlings, demonstrating that they grow independently of the antlers. An alternative functional significance of muntjac facial ridges correlates with certain particular behaviours in *Muntiacus*. It has been suggested that they have a protective function for the eyes against the use of double offensive weapons – antlers and tusks – in intraspecific combats (Croitor, 2014). Besides, a functional purpose related to the presence of the facial scent glands of muntjacs seems plausible. Muntjacs possess two pairs of facial scent glands, one frontal and one preorbital formed by very large glands, that are used for social communication and bonding. The facial ridges are located precisely between them. The frontal glands – not present in any other deer – are situated just along the medial borders of the facial ridges. The protective function of the ridges for these facial glands in relation to the bizarre opening (even eversion) and closing of the two sets of glands, has not been properly researched and presents a very plausible alternative explanation for the presence of anteorbital ridges that has no relation to the presence of cranial gear. In any case, the hypothesis of a direct unequivocal correlation between enlarged ante-preorbital regions and the presence of cranial appendages in ruminants as presented by Mennecart et al. (2021) can be safely rejected. Even admitting that the ante-supraorbital area in this specific fossil may be thickened, this condition cannot blindly be considered homologous to an actual cranial appendage of any kind, and has never been sustained as such by any previous publication. Besides, although the "prominent supraorbital ridges" (Mennecart et al., 2021, p. 17) described in PIMUZ A/V 4656 are somewhat similar to the facial crests of *Muntiacus*, they are far less developed. In fact the orbital edge is relatively thin, meaning that the 'crests' are in front of the orbits as ante-supraorbital structures, not above them (Fig. 6). The specimen PIMUZ A/V 4656 is broken and the posterior orbital region is missing, but taking into account that the upper orbital edge is not thickened it is highly unlikely that the 'crests' could reach the posterior region where the appendages should be positioned, following the comparison with *Muntiacus*. Moreover, the condition of PIMUZ A/V 4656 could be pathological. It is worth noting that, as pointed out by Mennecart et al. (2021), this skull has a clear bilateral pathological condition affecting both P4, left and right, which are missing just at the level where the anteorbital ridge ends. Finally, PIMUZ A/V 4656 shows no trace of small cranial protuberances similar to those of '*A*.' *xishuiensis* (Fig. 6, attachment areas of '*A*.' *xishuiensis* cranial gear superimposed to PIMUZ A/V 4656). Several cranial remains of European *Amphimoschus* have been recovered (Mennecart et al., 2021), including at least two complete skulls (e.g. MNHN.F.Ar3466 from Artenay and SMNS 40693 from Langenau), none showing thickened ante-supraorbital edges or anything similar to cranial headgear. It could be argued that SMNS 40693 is not a fully adult specimen and so could lack the facial ridges. However, in *Muntiacus* the facial ridges are present in both genders at a very young age (neonate-fawns, less than 2 months old), and if the hypothesis of the homology between these structures and the thickened supra-anteorbital of *Amphimoschus* is correct, the Langenau skull, pre-adult with erupted M2 and incipient M3, should have these structures present. On the other hand, MNHN.F.Ar3466 is a skull from an adult specimen (possibly a male due to its large sagittal keel), and, as in the case of SMNS 40693, it also lacks thickened ante-supraorbital regions. This anatomical evidence reinforces the notion that the ante-supraorbital condition of PIMUZ A/V4656 is very probably pathological (or at best a particular feature of that individual or its population), and cannot be considered apomorphic for *Amphimoschus*, much less as evidence of the presence of cranial headgear in this genus. Hence, the available evidence rejects the hypothesis of the presence of cranial appendages in the European 'real' *Amphimoschus*.

Amphimoschus was recently linked to the Bovoidea following the description of a sample of new cranial and dental material from China assigned to the new species *Amphimoschus xishuensis* (Y.-K. Li et al., 2021). These fossils include both upper and lower dentition together with a relatively poorly preserved skull

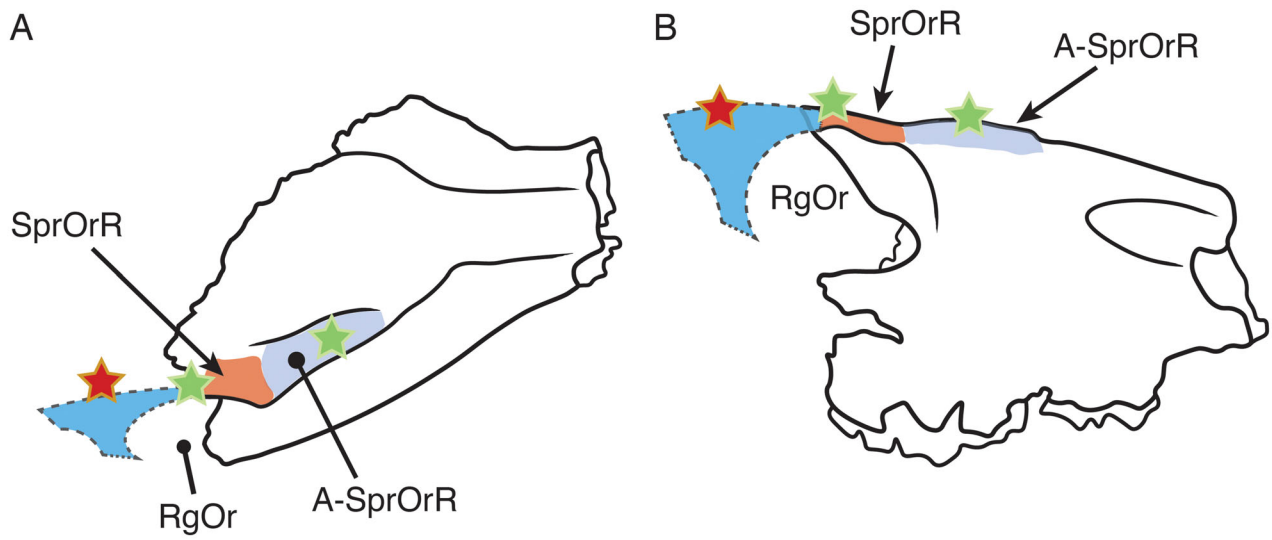

Fig. 6. Schematic of *Amphimoschus* skull PIMUZ A/V 4656 showing the thickened ante-supraorbital ridge and the thinner supraorbital region. The posterior region of the orbit, here represented with a dotted area filled in blue, is missing in the fossil. The green stars represent the placement points of *Dimidiomeryx xishuiensis* ('*A*.' *xishuiensis*) anteorbital and supraorbital 'bumps'. The red star represents the approximate placement point of primitive cranial appendages in forms like the basal bovid *Eotragus* and the point of placement of muntjac antlers. PIMUZ A/V 4656 shows no trace of cranial gear in the *Dimidiomeryx* positions. **Abbreviations**: **A-SprOrR**, ante-supraorbital ridge; **RgOr**, right orbit; **SprOrR**, supraorbital region.

characterized by having thickened frontal bones and facial area together with four small protuberances or bumps, two antorbital and two supraorbital, with thin corticals and thick spongy central regions, that Y.-K. Li et al. (2021) interpreted as a very primitive set of cranial appendages. This would be one of the earliest (19.7–17 Ma) examples of ruminant cranial headgear registered in the fossil record. The authors describe these bumps as "possible cranial horn-like appendages between developmental stage C2 and C3 of Bubenik (1990)" (Y.-K. Li et al., 2021, p. 9) but in a fully adult animal, which is a significant deviation from the ontogenetic interpretation that Bubenik (1990) gave to those stages. Although Y.-K. Li et al. (2021) did not specify any anatomically based hypothesis about the nature of '*A*.' *xishuiensis* 'proto-horns', the adjective 'horn-like' implies an epiphyseal character. In fact, examining the '*A*'. *xishuiensis* skull IVPP V 25521.2, it is possible to detect suture lines visible between the bump bases and the cranial roof, which are especially clear at the base of the right supraorbital bump (Y.-K. Li et al., 2021, fig. 2A and C). The computed tomography image provided by Y.-K. Li et al. (2021) also shows a clear line of contact between the bump bases and the cranial roof (Y.-K. Li et al., 2021, fig. 2B). Given the fully adult age of IVPP V 25521.2 demonstrated by its preserved dentition, these lines of contact indicate that these cranial appendages, if this is what they are, show a late attachment to the skull, thus confirming their similarities with giraffomorph ossicones and the knobs associated with secondary deposition of bony layers on the adult skulls of *Giraffa*. If really related to bovid horn origins, '*A*'. *xishuiensis* headgear would fit the 'proto-horn' hypothesis of Bubenik (1990), that considered an ossicone-like appendage as the earliest stage of horn evolution. Skull IVPP V 25521.2 preserves the major part of the anteorbital region of the rostrum, and contrary to the original description of Y.-K. Li et al. (2021), we consider that '*A*.' *xishuiensis* does not have an ethmoidal vacuity but shows a lacrimal fossa. The ethmoidal vacuity of ruminants is an open window in the anteorbital region of the rostrum, a literal hole or window going into the skull and delimited by several bones of the rostrum (lacrimal bone, nasal, maxilar, and the anterior part of the frontal bone). Despite its poor condition, the skull of '*A*.' *xishuiensis* fully preserves this region and the open window of the ethmoidal vacuity is totally missing (see Y.-K. Li et al., 2021, fig. 2). Also, it seems that '*A*.' *xishuiensis* presents a depression located in front of the orbit under the nasal 'ridge' that can be interpreted as a lacrimal fossa despite the strong deformation of the skull (see Y.-K. Li et al., 2021, fig. 2). The lower molars of '*A*'. *xishuensis* show the bovidomorph state of distolingual closing, with a total fusion of the post-entocristid and the post-hypocristid (our character 41:2) forming a single surface in which the two cristids are impossible to distinguish. This state involves not only the full fusion of the cristids but also constructional differences in the

lingual wall that are also visible in the images provided by Y.-K. Li et al. (2021). The lingual wall of the molars just behind the posterolingual closing lacks the slight slit present in molars with character state 41:1 and shows instead a single continuous wall, whilst the disto-lingual wall of molars with character state 41:1 have two 'parts' still visible corresponding to the unfused post-entocristid and post-hypocristid. Contrary to Y.-K. Li et al. (2021), this is not the condition of European *Amphimoschus*, in which the post-entocristid contacts or almost contacts the post-hypocristid but they are never fused (character 41:1). Y.-K. Li et al. (2021) recovered *Amphimoschus* (including '*A*'. *xishuiensis*) as the sister group of the clade formed by moschids and bovids, considering this entire lineage the Bovoidea (Y.-K. Li et al., 2021). However, their analysis was incorrect from a methodological and analytical cladistic standpoint. When testing the phylogenetic affinities of a new taxon, this taxon must be included as a separate terminal in the analysis. However, Y.-K. Li et al. (2021) assumed that both the European *Amphimoschus* and the new Chinese ruminant were the same taxon before including them, merged together, in the phylogenetic analysis, as a single taxonomic unit (the genus *Amphimoschus*). Hence, they never really tested the assignment of the Chinese four-horned pecoran to *Amphimoschus*. Here, we separated the classic European *Amphimoschus* on the one hand (including our new postcranial data) and '*A*'. *xishuensis* on the other to test their putative sister-group relationship as well as to test the cervoid-bovoid hypotheses for *Amphimoschus*. Our results not only rejected the bovoid nature of *Amphimoschus*, as we have previously discussed, but also confirmed the bovoid affinities of '*A*.' *xishuensis* – but as the direct sister group to bovids, not to moschids plus bovids as in Y.-K. Li et al. (2021). This is the first time that a new pecoran breaks the direct sister-group relationship of moschids and bovids within the Bovoidea since it was first proposed by Hassanin and Douzery (2003). Among other morphological traits, '*A*'. *xishuiensis* shares with bovids the absence of an ethmoidal vacuity and the presence of a lacrimal fossa located in front of the lacrimal orifice. More research is needed to better comprehend the nature of the cranial gear of this strange crown pecoran – hereby renamed *Dimidiomeryx xishuiensis* (Y.-K. Li, Mennecart, Aiglstorfer, Ni, Li, & Deng, 2021) – and its potential involvement in bovid horn origins.

The hornless pecorans *Dremotherium*, *Blastomeryx* and *Namibiomeryx* are recovered forming a lineage on their own (Fig. 5; also see Sánchez, Cantalapiedra, et al., 2015, fig. 9). This clade is the sister group of cervoids, forming with them the inclusive lineage of crown pecorans that we name the Cervidomorpha. The reconstructed morphological synapomorphies (Tables 2–3) that diagnose the Cervidomorpha are: presence of lacrimal fossa located in front of the lacrimal orifice(s); parieto-squamosal suture in the middle of the temporal fossa; and p4 with mesolingual conid joining the cristid obliqua through the postero-lingual cristid. The Cervidomorpha is here defined as the least inclusive clade of crown pecorans containing *Namibiomeryx* and the Cervidae. Cervidomorphs, of which extant deer are the only living representatives, are also – like bovidomorphs and giraffomorphs – truly ancient. Cervidomorphs were highly successful during the Miocene, since at the beginning of the Middle Miocene they lived in Africa, Eurasia and North America. More taxa (e.g. lagomerycids, hoplitomerycids and some hornless forms such as *Tuscomeryx*, *Friburgomeryx*, *Pomelomeryx*, *etc*.) need to be analysed to fully comprehend the evolution and composition of cervidomorphs/cervoids. One question that will need to be addressed is whether *Amphimoschus* constitutes a separate lineage of cervoids or instead is closely allied with some other lineage. In this regard, some authors (Janis & Scott, 1987; Leinders, 1983; Mazza & Rustioni, 2011) linked *Amphimoschus* to the Hoplitomerycidae, including it in this family of insular enigmatic multi-horned pecorans. Some *Hoplitomeryx* traits – e.g. presence of a slit-like elliptical opening in the border of the mastoid-occipital suture and the morphology of metatarsal III–IV – could indicate cervoid affinities, although recent claims against the cervoid nature of *Hoplitomeryx* have been made (Mazza, 2013). Hence, it should be tested whether hoplitomerycids are cervoids and if *Amphimoschus* is directly related to them.

Despite being hornless, *Amphimoschus* is a derived pecoran, not only regarding its synapomorphic cervoid cranial and postcranial features but also because of its high number of cranial, dental and postcranial autapomorphic traits. Interestingly enough, Mennecart et al. (2021) showed that some features of the inner ear of *Amphimoschus* – e.g. cochlea showing a high number of coils among others – are also very derived compared to Miocene cervids and other contemporaneous ruminants. Also, *Amphimoschus* has relatively high-crowned molars with developed cristids/cristae, and a bicuspid third lobe of the m3 developed in parallel with moschids. (see also Mennecart et al., 2021).

The differences present in the metatarsals III–IV and navicular-cuboids from Artenay and Pontlevoy involve both size and morphology in a pattern that points to the presence of two groups of European *Amphimoschus*. The hypothesis of a single species of *Amphimoschus* raised by Mennecart et al. (2021) was exclusively based on dental characters, but all ruminants evolve as

mosaics. The addition of these postcranial differences to the consideration of the variability of *Amphimoschus* in Europe clearly calls into question the validity of *A. artenensis* Mayet, 1908 as a separate species.

The hornless condition of *Amphimoschus* and the lack of horned forms at the base of the Cervidomorpha adds complexity to the single/multiple debate on the origin of pecoran headgear. As pointed out by Davis et al. (2011), there are many known hornless pecorans in the fossil record, and resolving their phylogenetic position within the pecoran tree is critical to test the competing hypotheses about the origin of pecoran cranial appendages. The genetic potential to develop cranial appendages from neural crest cells can be considered a deep molecular homology of crown pecorans (Y. Wang et al., 2019). However, when the presence/absence of headgear is plotted over a phylogenetic tree including fossils (Fig. 7), many independent losses would need to be reckoned if a single origin for the cranial appendages (following Y. Wang et al., 2019) is considered. This is so even if the single origin is hypothesized at the base of crown Pecora (Fig. 7, position 2), the less inclusive option that strictly follows Y. Wang et al. (2019). On the other hand, the absence of horned stem pecorans means the hypothesis of the single origin at the base of the Pecora (Fig. 7, position 1) is highly unlikely. We need to add more hornless pecoran taxa to total-evidence analyses to further test the single origin of pecoran headgear in a deep-time context with the fossil record. We may be faced with a scenario that confronts the phenotypic expression of headgear (accounted for in both the fossil record and the extant forms) *vs* the

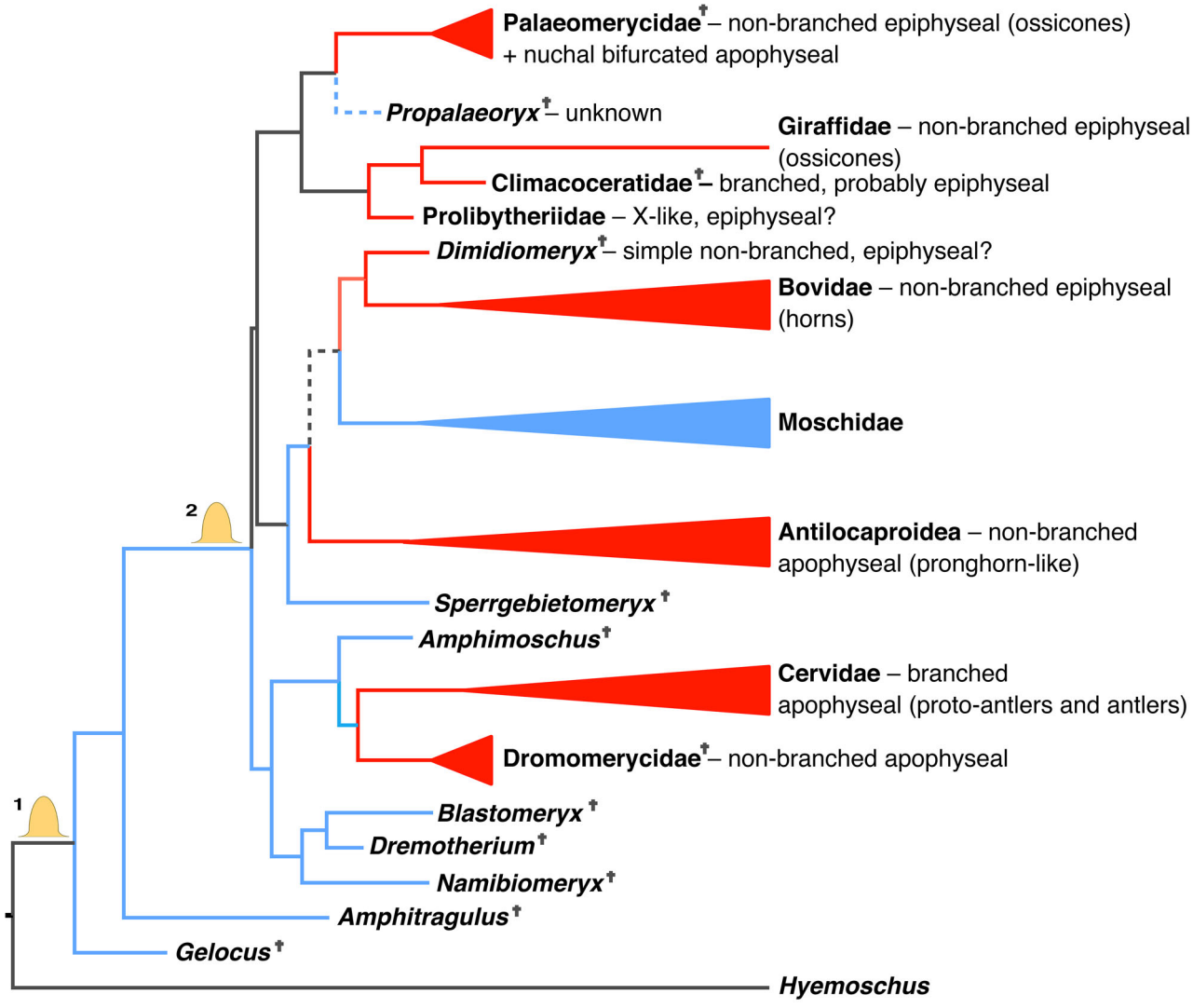

Fig. 7. Mapping of the presence of headgear among pecoran lineages across Tree 2. **1**, possible ancestral single origin of pecoran headgear at the base of Pecora; **2**, possible ancestral single origin of pecoran headgear at the base of crown Pecora.

genetic potential to express headgear (which does not necessarily imply the actual presence of cranial appendages and thus cannot be accounted for in fossils), as already proposed by Bubenik (1990).

The postcranial skeleton of *Amphimoschus*

The appendicular anatomy of *Amphimoschus* is significantly different from that of bovids and cervids. In Artenay, *Amphimoschus* appears together with the cervid *Procervulus dichotomus* and the bovid *Eotragus artenensis*, and in Aérotrain with *Procervulus dichotomus* and *Eotragus* cf. *clavatus* (Ginsburg, 1990). In Pontlevoy *Amphimoschus* is found together with three deer that are almost indistinguishable in their postcranial size and morphology: *Procervulus dichotomus*, *Dicrocerus elegans parvicerus* and *Paradicrocerus elegantulus* (Ginsburg, 1990). The remaining fossil pecorans from these three sites (the stem pecoran *Amphitragulus*, lagomerycids and palaeomerycids) are either too large or too small to be confused with *Amphimoschus*. *Procervulus* characters here discussed can be reviewed in Ginsburg and Bulot (1987) and Rössner (1995). The distal closing of the metatarsal sulcus and the cervid-type canal for the common digital artery clearly separates the metatarsal III–IV of *Amphimoschus* from bovid metatarsals, which have a distally open metatarsal sulcus and in the case of *Eotragus* a moschid-type canal for the digital common artery (see Sánchez et al., 2010). The navicular-cuboid of *Amphimoschus* has a cervid-like plantar surface with presence of a round crest that develops in the distal part of the plantomedial process and a slightly developed central canal (characters 63:1, 64:1), very different from the derived bovoid state without crests and central canal (characters 63:0, 64:0; Sánchez et al., 2010; Sánchez, Cantalapiedra, et al., 2015). Very little has been published about the postcranial skeleton of *Eotragus*, but morphologically the slender phalanges of *Amphimoschus* are totally different from the 'regular' shorter phalanges of *Eotragus* (Crouzel, 1971) and other basal bovids such as *Namacerus* (Morales et al., 2003). This is very noticeable in the first and second phalanges. More similarities between cervids and *Amphimoschus* could be expected; however, the appendicular skeleton of *Amphimoschus* has a very distinctive set of morphological features. The morphology of the proximal surface of the metatarsal III–IV of *Amphimoschus* (see description) is very different from that of cervids, which lack the double facet for the entocuneiform and the plantar portion of the proximal metatarsal articular surface clearly differentiated from the dorsal portion by lateral and medial incisures. In *Amphimoschus* the metatarsal sulcus closes higher above the distal pulleys of the metatarsal III–IV. The distal profile of the metatarsal III–IV is more angular in *Procervulus* (it is very rounded in *Amphimoschus*), with the insertions for the collateral ligaments more marked than in *Amphimoschus*. Also, the distal dorsal profile of the metatarsal III–IV is more markedly convex in *Amphimoschus*, and the supra-articular grooves are more marked than in *Procervulus*. In proximal view, this same bone has a more marked furrow for the extensor ligament in *Amphimoschus*. The sulcus of the metacarpal III–IV closes higher in *Procervulus* than in *Amphimoschus* (contrary to the metatarsal III–IV). The distal profile of the metacarpal III–IV in dorsal view is sub-triangular in *Procervulus*, with strongly marked insertions for the collateral ligaments, but is straighter in *Amphimoschus*, with the insertions for the collateral ligaments barely developed. The lateral lobe of the distal trochlea of the astragalus of *Procervulus* is clearly higher than the medial one. However, the two lobes are equal in *Amphimoschus*. Also, the dorsal keel of the medial lobe in the proximal trochlea is straight in *Amphimoschus* but laterally inclined in *Procervulus*. In dorsal view, the proximal articular facets of the radius have a marked lateral and medial inclination in *Procervulus*; however, they are more horizontal in *Amphimoschus*. The radius is more slender and elongated in *Amphimoschus* compared to *Procervulus*. The first phalanx is more elongated in *Amphimoschus* than in *Procervulus*. And the third phalanx of *Amphimoschus* is a very modified and elongated version of a Köhler Type A phalanx (Köhler, 1993) very different from the regular Type A of *Procervulus* (Ginsburg & Bulot, 1987; Rössner, 1995).

The autopodial morphology of *Amphimoschus* is highly specialized and offers insights on its habitat preferences. The *Amphimoschus* autopodium shows sprawling first and second phalanges complemented by very long and flattened third phalanges with enlarged ventral surfaces (Fig. 8). Among living pecorans, a similar suite of derived features appears in the extant moschids *Moschus* spp. and the African sitatungas, a group of semiaquatic bovids in the genus *Tragelaphus* (*T. spekii*, *T. larkenii*, *T. selousi* and *T. gratus*). Musk deer and sitatungas walk with almost flattened digits that expand the surface of contact of the animal with the ground, also deflecting the body weight when the autopodium hits the ground (Köhler, 1993). Musk deer have digits that sprawl at a 35° angle and when walking on soft ground or snow they make use of the entire interdigital surface, not only the digits (Prikhod'ko, 2012, personal communication). Similar to these two extant bovoids, *Amphimoschus* digits surely sported long and ventrally flat keratinous sheaths covering the third phalanges to increase the autopodial support area. Also, *Amphimoschus* had a digital angle very similar to that of *Moschus* (Fig. 8). This set of features is probably

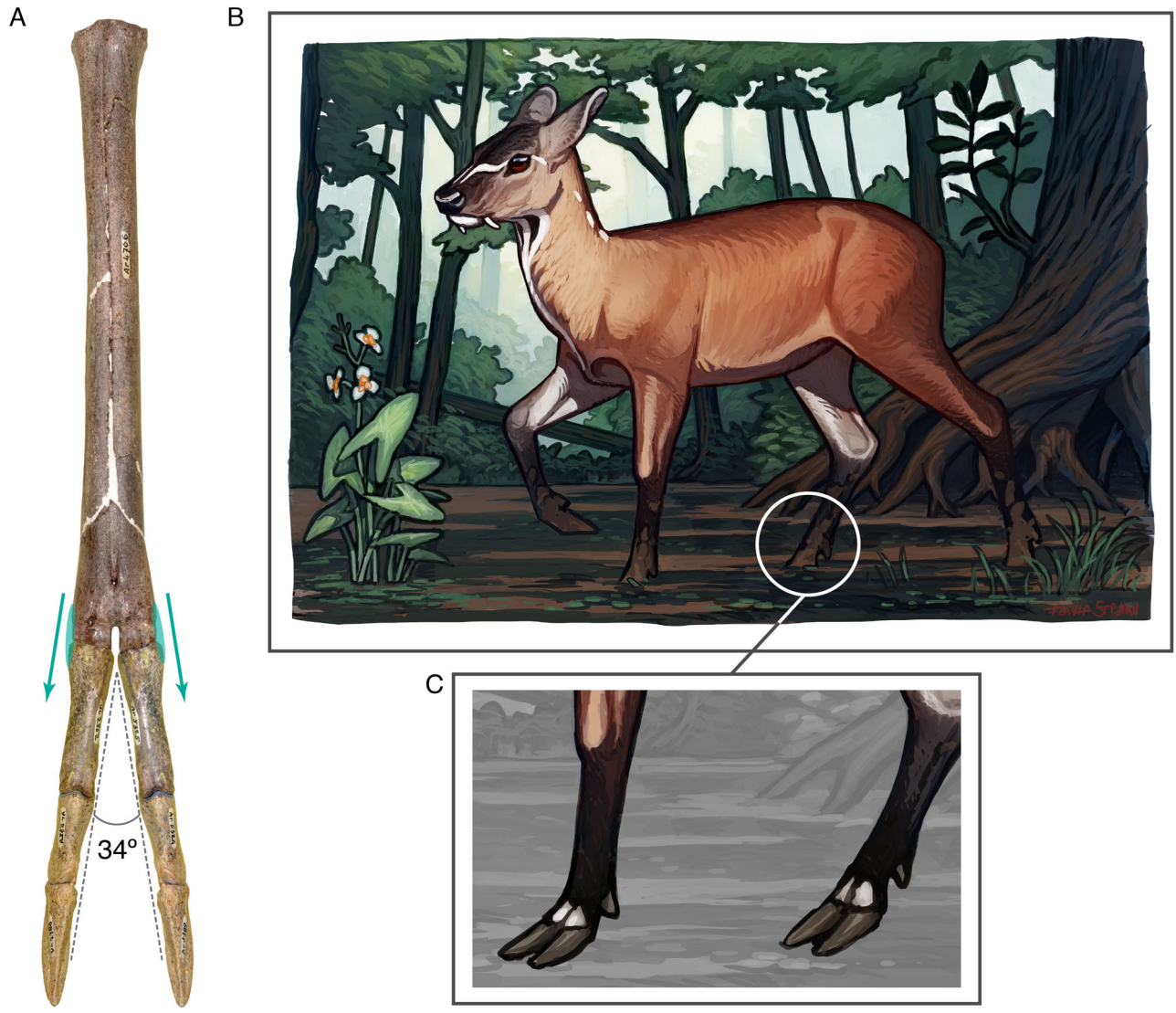

Fig. 8. *Amphimoschus*, autopodial morphology and palaeoecological implications. **A**, composite articulated right anterior autopodium of *Amphimoschus* from Artenay (right digit mirrored from the single preserved one) showing the *c*. 34° angle formed by *Amphimoschus* digits (similar to extant *Moschus*), with digits in neutral articulation position and the collateral ligaments (marked in green) showing the vector of their action (green arrows); **B**, reconstruction of an adult male *Amphimoschus* in its postulated habitat; **C**, detail of *Amphimoschus* left manus and right pes showing the elongated sitatunga-like main hooves and the flat stance of the digits III–IV against the ground. Art by Flavia Strani.

highly specialized. It has been hypothesized that the sprawling autopodial morphology with long, flat third phalanges appears in ruminants that inhabit wooded moistened habitats (Köhler, 1993; Leinders, 1979). The sprawling digits serve sitatungas well in their semi-aquatic/swampy habitats, preventing these bovids from sinking into the soft muddy ground full of vegetation mats. However, they have more difficulty when moving on harder ground (Groves & Leslie Jr, 2011). On the other hand, musk deer use the sprawling autopodial morphology to achieve a high diversity of tasks: gripping in rocky terrain with the aid of very elongated side digits that almost touch the ground (these are unknown in *Amphimoschus*); walking on the very soft ground typical of the forests they inhabit; walking on snow, resting all the interdigital surfaces and the four digits on the snow crust; 'grabbing' low branches with the aid of the long side digits, after rearing on the hind legs, to nip at lichens and leaves; and climbing trees also with help of those lateral digits – directed to the sides – that transform *Moschus* autopodia into small strange 'hands' and 'feet' (Groves, 2011; Prikhod'ko,

2003, 2012). Hence, although it is clear that the sprawling autopodial configuration is linked to the exploitation of habitats with muddy/soft/plastic ground – this could be considered its basal role – extant musk deer demonstrate that is not limited to it. A great difference between sitatungas and *Moschus*, apart from their habitat, is their body size. Extant musk deer range between 6 and 18 kg (Groves, 2011) whereas the body mass of sitatungas ranges between 50 and 57 kg for females and between 75 and 125 kg for males (Groves & Leslie Jr, 2011). Probably, the wide functional spectrum associated with the sprawling autopodial morphology in *Moschus* is an exaptation based on the basic physical capacities of the sprawling-digits morphology in a very small and light animal. Our estimated body weight for *Amphimoschus* is about 36 kg (Table 1), a figure way up the upper range of *Moschus* spp. of *Moschus* spp. and below the range of *T. spekii*. Besides possessing elongated second phalanges that *Amphimoschus* lacks, several anatomical differences between *Moschus* and *Amphimoschus* come from the distal part of the metapodials, encompassing the dorsal and palmar/plantar development of the distal articulation keels, the depth of the internal half of each trochlea, and the development of the insertion tubercles for the collateral ligaments. The metacarpal III–IV of *Moschus* has keels more dorsally developed than *Amphimoschus*, and with deeper internal trochleae. Also, the tubercles for the insertion of the collateral ligaments are more projected in *Moschus*, hence these short ligaments – connecting the distal part of the metapodials to the proximal part of the first phalanges for preventing dislocation (Köhler, 1993) – are arranged at a more angled axis in *Amphimoschus* than in *Moschus*. These two features alone probably allowed *Amphimoschus* to spread its digits even more than *Moschus* could. The supra-articular fossae in the metacarpal III–IV are more developed in *Moschus* than in *Amphimoschus*, pointing to a lesser degree of flexion of the first phalanx in the latter. However, the supra-articular fossae of the metatarsal III–IV are similarly developed in *Moschus* and *Amphimoschus*, meaning that the latter could exert a similar charge of elastic potential energy in the hind limbs to propel the body forward when running. Extant musk deer are able to jump at high speed on both soft and rocky ground to escape predators (Groves, 2011; Prikhod'ko, 2003). The dorsally weaker distal keels of *Amphimoschus* metacarpals, together with their relatively less developed metacarpal supra-articular fossae, probably indicate a lower ability of *Amphimoschus*, if compared with *Moschus*, to rebound with the front limbs at high speed whilst transmitting the impulse produced by the hind limbs. Thus, *Amphimoschus* had probably less high-speed jumping capacity than *Moschus*. Furthermore, the third phalanx of *Amphimoschus* is relatively even more elongated than that of *Moschus*, and with the keratinous sheaths included, the relative surface of its spreading autopodium was comparatively larger, such that they were capable of walking over very soft/wet ground. Sitatungas have metacarpals III–IV more similar in these regards to *Amphimoschus* than to *Moschus*, having shallow trochleas, weak tubercles for the collateral ligaments in the metacarpal III–IV, poorly developed supra-articular fossae, and poorly developed keels, these two last features also indicating lesser high-speed jumping skills than *Moschus*. Similarly to *Amphimoschus*, sitatungas also have non-elongated second phalanges, in both the fore and hind limbs. In the metatarsals III–IV, the insertion areas for the collateral ligaments are more marked in sitatungas and *Moschus* than in *Amphimoschus*. The distal keels are very extended in *Moschus* on the palmar/plantar side of the metapodials, whereas in *Amphimoschus* and sitatungas they barely protrude over the border of the articular surface. This is a highly specialized character of extant *Moschus*. Finally, another analogous feature developed by both *Amphimoschus* and the sitatungas is the relative length of metacarpal III–IV and metatarsal III–IV. Contrary to *Moschus*, in which the metacarpals are clearly shorter than the metatarsals, *Amphimoschus* and sitatungas have elongated metacarpals III–IV that are only slightly shorter than the metatarsals III–IV. This 'stilted' long-legged configuration is surely advantageous in a wet/muddy/semiaquatic environment. Taking into account all the morphofunctional appendicular analogies between *Amphimoschus* and the sitatungas, it can be hypothesized that the former was a ruminant more ecologically akin to a smaller sized sitatunga than to a larger bodied version of the highly versatile *Moschus*, and thus an inhabitant of semiaquatic or swampy habitats (Fig. 8). This sitatunga-lifestyle is in line with the palaeocological description of the basins from where *Amphimoschus* is known. For example, the German Molasse Basin was described as a wetland with areas of marsh, peatlands, forests and fresh water that formed ponds and flowed into the main river or its tributaries (Eronen & Rössner, 2007; Kaiser & Rössner, 2007 and references therein). There, *Amphimoschus* has already been labelled as a browser (Kaiser & Rössner, 2007). Tragulids, also closely linked to forested wetlands and permanent water bodies, equally thrived in the Molasse Basin, even successfully competing with pecorans (Rössner, 2004). Also, macromammals associated with permanent water bodies and forested habitats (e.g. beavers) have been identified from the French sites of the Loire Basin that produced *Amphimoschus* remains,

including Artenay, Aérotrain and Pontlevoy (Ginsburg, 1990).

Conclusions

Part of the postcranial skeleton of the hornless Miocene pecoran ruminant *Amphimoschus* is comprehensively described here for the first time in 150 years on the basis of fossil material that comes from several Early and Middle Miocene French sites of the Loire Basin (Aérotrain, MN4; Artenay, MN4; and Pontlevoy, MN5). The sample comprises several elements of the appendicular skeleton.

This new material is key to deciphering the phylogenetic relationships of *Amphimoschus* within the Pecora. A suite of three Bayesian tip-dating analyses of total-evidence data sets recover *Amphimoschus* as the basal offshoot of a monophyletic Cervoidea, thus rejecting its purported affinities with the Bovoidea. Albeit hornless, *Amphimoschus* is a highly autapomorphic pecoran, very derived in many ways. The three main clades of crown pecorans (Cervidomorpha, Bovidomorpha and Giraffomorpha) are very inclusive lineages that probably diverged at some point around the middle–late Oligocene, producing the main lines leading to the extant pecoran diversity. Cervidomorphs were especially successful during the first part of the Miocene. The recently described '*Amphimoschus*' *xishuiensis* from the late Early Miocene of China appears here as the closer sister group to the Bovidae. Hence, we reject its previous assignment to the genus *Amphimoschus* and erect for it the new genus *Dimidiomeryx*, resulting in the new combination *D. xishuiensis* (Y.-K. Li, Mennecart, Aiglstorfer, Ni, Li, & Deng, 2021). The quadruple diminutive headgear of *Dimidiomeryx* is probably epiphyseal and ossicone-like, but more research is needed to assess its nature and its potential link with bovid horn origins.

The hypothesis of a direct unequivocal correlation between enlarged/thickened ante-preorbital regions such as the one present in the *Amphimoschus* skull PIMUZ A/V 4656 and the presence of cranial appendages in ruminants is rejected. The condition of the muntjac deer is very probably apomorphic. PIMUZ A/V 4656 presents thickened ante-supraorbital 'ridges' that do not continue into the thin supraorbital region, making it extremely unlikely that the ridges could continue into a supraorbital appendage as occurs in *Muntiacus*. Also, the lack of ante-supraorbital thickening in the skulls SMNS 40693 and MNHN.F.Ar3466, together with the clear bilateral pathological condition affecting both P4 in PIMUZ A/V 4656, makes it highly probable that the unique ante-supraorbital features of this skull also have a pathological origin. Hence, since no headgear can be identified in any known *Amphimoschus* skull, this genus should be considered hornless.

The lack of any horned forms at the base of the Cervidomorpha adds complexity to the debate about the single/multiple origin of pecoran cranial appendages. More hornless pecoran taxa need to be added to total-evidence data sets to further test the single origin of pecoran headgear in a deep-time context using the fossil record.

The slender and distinctive appendicular skeleton of *Amphimoschus* is clearly different from that of contemporaneous similarly sized pecorans (i.e. bovids and cervids) and gives us hints about the previously unknown ecological preferences of this crown pecoran. *Amphimoschus*, which had a body mass of around 36 kg, possessed a highly specialized appendicular morphology that was morphofunctionally very similar to that of extant sitatunga bovids, including the distal morphology of the metapodials, the long, spread-out digits with long and broad-based third phalangues, and a stilted long-legged limb configuration with metacarpals III–IV that were almost as long as the metatarsals. As occurs with modern sitatungas, *Amphimoschus* probably favoured forested muddy/swampy/semiaquatic habitats, relying on its long legs and wide-spreading digits to deflect its body weight when the autopodia hit the soft/wet ground during locomotion.

Acknowledgements

This publication was supported by the projects PID2020-116220GB-I00 and PID2020-117289GB-I00 funded by MCIN/AEI/10.13039/501100011033/, the Government of Aragón (Research Group ref. E33_23R), the CERCA Programme/Generalitat de Catalunya, and the research groups CSIC 641538 and CAM-UCM 910607. JLC acknowledges a Universidad de Alcalá Grant 2017-T1/AMB5298 and the Talent Attraction Program of the Madrid Government. FS is a 'Juan de la Cierva Formación' fellow (ref. FJC2020-042982-I) funded by MCIN (MCIN/AEI/10.13039/501100011033) and the European Union "NextGenerationEU/PRTR" program. We thank Bastien Mennecart and Loïc Costeur for past comments and interesting discussions on *Amphimoschus* systematics. We are grateful to the curatorial staff of the MNHN (Paris) that loaned the fossils to us. We also thank Francisco Pastor (Museo Anatómico de la Universidad de Valladolid, Valladolid, Spain) for providing the sitatunga postcranial material used in this work, and Pablo Amado for the help with the Latin language. Finally, we dedicate this work to the

memory of Leonard Ginsburg and M[a] Dolores Soria, who started this research on the postcranial skeleton of *Amphimoschus* long ago.

Disclosure statement

No potential conflict of interest was reported by the author(s).

Supplemental material

Supplemental material for this article can be accessed here: https://doi.org/10.1080/14772019.2024.2386020.

ORCID

Israel M. Sánchez http://orcid.org/0000-0003-2151-7693
Juan L. Cantalapiedra http://orcid.org/0000-0003-0913-7735
Daniel DeMiguel http://orcid.org/0000-0001-6138-7227
Beatriz Azanza http://orcid.org/0000-0003-2487-547X
Flavia Strani http://orcid.org/0000-0003-4566-3644
Jorge Morales http://orcid.org/0000-0001-5170-5754

References

Bibi, F., Bukhsianidze, M., Gentry, A. W., Geraads, D., Kostopoulos, D. S., & Vrba, E. S. (2009). The fossil record and evolution of Bovidae: State of the field. *Palaeontologia Electronica*, *12*, 1–11.

Bouckaert, R., Heled, J., Künert, D., Vaughan, T. G., Wu, C.-H., Xie, D., Suchard, M. A., Rambaut, A., & Drummond, A. J. (2014). BEAST2: A software platform for Bayesian evolutionary analysis. *PLoS Computational Biology*, *10*, e1003537. https://doi.org/10.1371/journal.pcbi.1003537

Bourgeois, L.-A. (1873). Note sur l'*Amphimoschus ponteleviensis*. *Journal de Zoologie*, *2*, 235–236.

Bubenik, A. B. (1990). Epigenetical, morphological, physiological, and behavioral aspects of evolution of horns, pronghorns, and antlers. In G. A. Bunenik & A. B. Bubenik (Eds.), *Horns, pronghorns, and antlers: Evolution, morphology, physiology, and social significance* (pp. 3–113). Springer-Verlag.

Chen, L., Qiu, Q., Jiang, Y., Wang, K., Lin, Z.-S., Li, Z.-P., Bibi, F., Yang, Y.-Z., Wang, J.-H., Nie, W.-H., Su, W.-T., Liu, G.-C., Li, Q.- Y., Fu, W.-W., Pan, X.-Y., Liu, C., Yang, J., Zhang, C.-Z., Yin, Y., … Wang, W. (2019). Large-scale ruminant genome sequencing provides insights into their evolution and distinct traits. *Science*, *364*, eaav6202. https://doi.org/10.1126/science.aav6202

Coope, G. R. (1968). The evolutionary origin of antlers. *Deer*, *1*, 215–217.

Croitor, R. (2014). Deer from Late Miocene to Pleistocene of Western Palearctic: matching fossil record and molecular phylogeny data. *Zitteliana B*, *32*, 115–153.

Crouzel, F. (1971). Sur les squelettes entiers et les ensembles d'ossements en connexion, trouvés a Sansan (Helvétien moyen du Gers). *Comptes Rendus du 96ème congrès national des Sociétés savants*, *Paris*, t. 2, 157–170.

Davis, E. B., Brakora, K. A., & Lee, A. H. (2011). Evolution of ruminant headgear: A review. *Proceedings of the Royal Society B*, *278*, 2857–2865. https://doi.org/10.1098/rspb.2011.0938

DeMiguel, D. (2016). Disentangling adaptive evolutionary radiations and the role of diet in promoting diversification on islands. *Scientific Reports*, *6*, 29803. https://doi.org/10.1038/srep29803

DeMiguel, D., Quiralte, V., Azanza, B., Montoya, P., & Morales, J. (2012). Dietary behaviour and competition for vegetal resources in two Early Miocene pecoran ruminants from Central Spain. *Geodiversitas*, *34*, 425–443. https://doi.org/10.5252/g2012n2a10

Eronen, J., & Rössner, G. E. (2007). Wetland paradise lost: Miocene community dynamics in large herbivorous mammals from the German Molasse Basin. *Evolutionary Ecology Research*, *9*, 471–494.

Gentry A. W. (1994). The Miocene differentiation of Old World Pecora (Mammalia). *Historical Biology*, *7*, 115–158. https://doi.org/10.1080/10292389409380449

Gentry, A. W. (2000). The ruminant radiation. In E. S. Vrba & G. B. Schaller (Eds.), *Antelopes, deer, and relatives: Fossil record, behavioral ecology, systematics and conservation* (pp. 11–45). Yale University Press.

Gentry, A. W., & Hooker, J. J. (1988). The phylogeny of the Artiodactyla. In M. J. Benton (Ed.), *Phylogeny and classification of the tetrapods*, *Vol. 2: Mammals* (pp. 235–272). Clarendon Press.

Gentry, A. W., Rössner, G. E., & Heizmann, E. P. J. (1999). Suborden Ruminantia. In G. E. Rössner & H. K. Heisig (Eds.), *The Miocene land mammals of Europe* (pp. 225–253). Verlag Dr Friedrich Pfeil.

Geraads, D., Bouvrain, G., & Sudre, J. (1987). Relationships phyletiques de *Bachitherium* Filhol, ruminant de L'Oligocene d'Europe occidentale. *Palaeovertebrata*, *17*, 43–73.

Ginsburg, L. (1990). The faunas and stratigraphical subdivisions of the Orleanian in the Loire Basin (France). In E. H. Lindsay, V. Fahlbusch, & P. Mein (Eds.), *European Neogene mammal chronology* (pp. 157–176). Plenum Press and NATO Scientific Affairs Division.

Ginsburg, L., & Bulot, Ch. (1987). Les Artiodactyles sélénodontes du Miocène de Bézian à La Romieu (Gers). *Bulletin du Musèum national dHistoire naturelle, Paris*, *4*, 63–95.

Gray, J. E. (1821). On the natural arrangement of vertebrose animals. *The London Medical Repository Journal and Review*, *15*, 296–310.

Grimm, G. W., Kapli, P., Bomfleur, B., McLoughlin, S., & Renner, S. S. (2015). Using more than the oldest fossils: Dating Osmundaceae with three Bayesian clock approaches. *Systematic Biology*, *64*, 1–22. https://doi.org/10.1093/sysbio/syu108

Groves, C. P. (2011). Family Moschidae (musk-deer). In D. E. Wilson & R. A. Mittermeier (Eds.), *Handbook of the mammals of the World*. Volume *2: Hoofed mammals* (pp. 336–348). Lynx Edicions.

Groves, C. P., & **Leslie Jr, D. M.** (2011). Bovidae (hollow-horned ruminants). In D. E. Wilson & R. A. Mittermeier (Eds.), *Handbook of the mammals of the world*. Volume *2: Hoofed mammals* (pp. 444–779). Lynx Edicions.

Guha, S., **Goyal, S. P., & Kashyap, V. K.** (2007). Molecular phylogeny of musk deer: A genomic view with mitochondrial 16S rRNA and cytochrome *b* gene. *Molecular Phylogenetics and Evolution*, *42*, 585–597. https://doi.org/10.1016/j.ympev.2006.06.020

Hamilton, W. R. (1978). Cervidae and Palaeomerycidae. In V. J. Maglio & H. B. S. Cooke (Eds.), *Evolution of African mammals* (pp. 496–508). Harvard University Press.

Hassanin, A., & Douzery, E. J. P. (2003). Molecular and morphological phylogenies of Ruminantia and the alternative position of the Moschidae. *Systematic Biology*, *52*, 206–228. https://doi.org/10.1080/10635150390192726

Hassanin, A., **Delsuc, F.**, **Ropiquet, A.**, **Hammer, C.**, **van Vuuren B. J.**, **Matthee, C.**, **Ruiz-García, M.**, **Cetzeflis, F.**, **Areskoug, V.**, **Nguyen, T. T., & Couloux, A.** (2012). Pattern and timing diversification of Cetartiodactyla (Mammalia, Laurasitheria), as revealed by a comprehensive analysis of mitochondrial genomes. *Comptes Rendus Biologies*, *335*, 32–50. https://doi.org/10.1016/j.crvi.2011.11.002

Janis, C. M. (1982). Evolution of horns in ungulates: Ecology and paleoecology. *Biological Reviews*, *57*, 261–318. https://doi.org/10.1111/j.1469-185X.1982.tb00370.x

Janis, C. M. (1986). Evolution of horns and related structures in hoofed mammals. *Discovery*, *19*, 9–17.

Janis, C. M. (1990a). The correlation between diet and dental wear in herbivorous mammals, and its relationship to the determination of diets of extinct species. In A. J. Boucot (Ed.), *Paleobiological evidence for rates of coevolution and behavioral evolution* (pp. 241–259). Elsevier.

Janis, C. M. (1990b). Correlation of cranial and dental variables with body size in ungulates and macropodoids. In J. Damuth & B. J. MacFadden (Eds.), *Body size in mammalian paleobiology* (pp. 255–300). Cambridge University Press.

Janis, C. M., & Scott, K. M. (1987). The interrelationships of higher ruminant families: With special emphasis on the members of the Cervoidea. *American Mueum Novitates*, *2893*, 1–85.

Kaiser, T. M., & Rössner, G. E. (2007). Dietary resource partitioning in ruminant communities of Miocene wetland and karst palaeoenvironments in Southern Germany. *Palaeogeography, Palaeoclimatoclogy, Palaeoecology*, *252*, 424–439. https://doi.org/10.1016/j.palaeo.2007.04.013

Köhler, M. (1993). Skeleton and habitat of recent and fossil ruminants. *Münchner Geowissenschaftliche Abhandlungen*, *25*, 1–88.

Lee, M. S. Y, & Worthy, T. H. (2012). Likelihood reinstates *Archaeopteryx* as a primitive bird. *Biology Letters*, *8*, 299–303. https://doi.org/10.1098/rsbl.2011.0884

Leinders, J. J. M. (1979). On the osteology and function of the digits of some ruminants and their bearing on taxonomy. *Zeitschrift Sängetierkunde*, *44*, 305–318.

Leinders, J. J. M. (1983). Hoplitomerycidae fam. nov. (Ruminantia, Mammalia) from Neogene fissure fillings in Gargano (Italy). Part 1: the cranial osteology of *Hoplitomeryx* gen. nov. and a discussion on the classification of pecoran families. *Scripta Geologica*, *70*, 1–68.

Leinders, J. J. M., & Heintz, E. (1980). The configuration of the lacrimal orifices in pecorans and tragulids (Artiodactyla, Mammalia) and its significance for the distinction between Bovidae and Cervidae. *Beaufortia*, *30*, 155–162.

Li, C. K., **Lin, Y. P.**, **Gu, Y. M.**, **Hou, L. H.**, **Wu, W. Y., & Qiu, Z. D.** (1983). The Aragonian vertebrate fauna of Xiacaowan, Jiangsu–1. A brief introduction to the fossil localities and preliminary report on the new material. *Vertebrata PalAsiatica*, *21*, 313–327.

Li, Y.-K., **Mennecart, B.**, **Aiglstorfer, M.**, **Ni, X.-J.**, **Li, Q., & Deng, T.** (2021). The early evolution of cranial appendages in Bovoidea revealed by new species of *Amphimoschus* (Mammalia: Ruminantia) from China. *Zoological Journal of the Linnean Society*, *20*, 1–15. https://doi.org/10.1093/zoolinnean/zlab053

Linnaeus, C. (1758). *Systema Naturae, Ed. X (Systema naturae per regna tria naturae, secundum classes, ordines, genera, species, cum characteribus, diferentiis, synonymis, locis. Tomus I. Editio decima reformata)*. Holmiae.

Marcot, J. D. (2007). Molecular phylogeny of terrestrial artiodactyls. Conflicts and resolution. In D. R. Prothero & S. E. Foss (Eds.), *The Evolution of Artiodactyls* (pp. 4–18). The Johns Hopkins University Press.

Mayet, L. (1908). Étude des mammifères miocènes des sables de l'Orleanais et des faluns de la Turaine. *Annales de l'Université de Lyon*, *NS24*, 1–336.

Mazza, P. P. A. (2013). The systematic position of Hoplitomerycidae (Ruminantia) revisited. *Geobios*, *46*, 33–42. https://doi.org/10.1016/j.geobios.2012.10.009

Mazza, P. P. A., & Rustioni, M. (2011). Five new species of *Hoplitomeryx* from the Neogene of Abruzzo and Apulia (Central and Southern Italy) with revision of the genus and of *Hoplitomeryx mattehi Leinders*, 1983. *Zoological Journal of the Linnean Society*, *163*, 1304–1333. https://doi.org/10.1111/j.1096-3642.2011.00737.x

McKenna, M. C., & Bell, S. K. (1997). *Classification of mammals above the species level*. Columbia University Press, New York.

Mennecart, B., **Dziomber, L.**, **Aiglstorfer, M.**, **Bibi, F.**, **DeMiguel, D.**, **Fujita, M.**, **Kubo, M.**, **Laurens, F.**, **Meng, J.**, **Métais, G.**, **Müller, B.**, **Ríos, M.**, **Rössner, G. E. Sánchez, I. M.**, **Schulz, G.**, **Wang, S., & Costeur, L.** (2022). Ruminant inner ear shape records 35 million years of neutral evolution. *Nature Communications*, *13*, 7222. https://doi.org/10.1038/s41467-022-34656-0

Mennecart, B., **Métais, G.**, **Costeur, L.**, **Ginsburg, L., & Rössner, G. E.** (2021). Reassessment of the enigmatic ruminant Miocene genus *Amphimoschus* Bourgeois, 1873 (Mammalia, Artiodactyla, Pecora). PLOS ONE, *16*, e0244661. https://doi.org/10.1371/journal.pone.0244661

Methner, K., **Campani, M.**, **Fiebig, J.**, **Löffler, N.**, **Kempf, O., & Mulch, A.** (2020). Middle Miocene long-term continental temperature change in and out of pace with marine climate records. *Scientific Reports*, *10*, 7989. https://doi.org/10.1038/s41598-020-64743-5

Montgelard, C., **Catzeflis, F., & Douzery, E.** (1997). Phylogenetic relationships of artiodactyls and cetaceans as deduced from the comparison of cytochrome *b* and 12S rRNA mitochondrial sequences. *Molecular Biology*

and Evolution, *14*, 550–559. https://doi.org/10.1093/oxfordjournals.molbev.a025792

Morales, J., Pickford, M., & Soria, D. (1993). Pachyostosis in a lower Miocene giraffoid from Spain, *Lorancameryx pachyostoticus* nov. gen. nov. sp. and its bearing on the evolution of bony appendages in artiodactyls. *Geobios*, *26*, 207–230. https://doi.org/10.1016/S0016-6995(93)80016-K

Morales, J., Soria, D., Pickford, M., & Nieto, M. (2003). A new genus and species of Bovidae (Artiodactyla, Mammalia) from the early Middle Miocene of Arrisdrift, and the origins of the family Bovidae. *Memoir of the Geological Survey of Namibia*, *19*, 371–384.

Mörs, T., von der Hocht, F., & Wutzler, B. (2000). Die erste Wirbeltierfauna aus der miozänen Braunkhole der Niederrheinischen Bucht (Ville-Schichten, Tagebau Hambach). *Paläontologische Zeitschrift*, *74*, 145–170. https://doi.org/10.1007/BF02987958

Nieto, M., Morales, J., Soria, D., Azanza, B., Gisnburg, L., Montoya, P., Peláez-Campomanes, P., Pickford, P., Lapparent de Broin, F., Quiralte, V., & Sánchez I. M. (2004). Origin of ruminant cranial appendages: Biochronological and biogeographical aspects. *Journal of Morphology*, *260*, 316.

Pilgrim, G. E. (1941). The dispersal of the Artiodactyla. *Biological Review*, *16*, 134–163. https://doi.org/10.1111/j.1469-185X.1941.tb01098.x

Pilgrim, G. E. (1946). The evolution of the buffaloes, oxen, sheep and goats. *Zoological Journal of the Linnean Society*, *41*, 272–286. https://doi.org/10.1111/j.1096-3642.1940.tb02077.x

Prikhod'ko, V. I. (2003). *Kabarga: proiskhozhdenie, sistematika, ekologiya, povedenie i kommunikaziya*. [*Musk deer: Origins, taxonomy, ecology, behavior and communication*]. GEOS.

Prikhod'ko, V. I. (2012). *Evolyuziya kabargovykh: morphologicheskie, molekulyarno-geneticheskie, etologicheskie i ecologicheskie aspekty* [*Evolution of Moschidae: Morphological, molecular-genetic, ethological and ecological aspects*]. KMK Scientific Press.

Prothero, D. R. (2007). Family Moschidae. In D. R. Prothero & S. E. Foss (Eds.), *The evolution of artiodactyls* (pp. 221–226). The Johns Hopkins University Press.

Qiu, Z.-X., & Qiu, Z.-D. (2013). Early Miocene Xiejiahe and Sihong fossil localities and their faunas, Eastern China. In X.-M. Wang, L. J. Flynn, & M. Fortelius (Eds.), *Fossil mammals of Asia: Neogene biostratigraphy and chronology* (pp. 142–154). Columbia University Press.

Qiu, Z.-X., Qiu, Z.-D., Deng, T., Li, C.-K., Zhang, Z.-Q., Wang, B.-Y., & Wang, X.-M. (2013). Neogene land mammal stages/ages of China: Toward the goal to establish abd Asian land mammal stage/age scheme. In X.-M. Wang, L. J. Flynn, & M. Fortelius (Eds.), *Fossil mammals of Asia: Neogene biostratigraphy and chronology* (pp. 29–90). Columbia University Press.

Rambaut, A., & Drummond, A. J. (2016). Tracer v. 1.6. Edinburgh: Institute of Evolutionary Biology, University of Edinburgh. http://beast.bio.ed.ac.uk/Tracer

Roman, F., & Viret, J. (1934). La faune de mmamifères du burdigalien de La Romieu. *Mémoires de la Sociéte Géologique de France*, *NS21*, 5–67.

Romer, A. S. (1966). *Vertebrate paleontology*. University of Chicago Press.

Ronquist, F., Klopfstein, S., Vilhemsen, L., Schulmeister, S., Murray, D. L., & Rasnitsyn, A. P. (2012). A total-evidence approach to dating with fossils, applied to the early radiation of the Hymenoptera. *Systematic Biology*, *61*, 973–999. https://doi.org/10.1093/sysbio/sys058

Rook, L., Abbazi, L., & Engesser, B. (1999). An overview on the Italian Miocene land mammal faunas. In J. Agustí, L. Rook, & P. Andrews (Eds.), *The evolution of Neogene terrestrial ecosystems in Europe* (pp. 191–204). Cambridge University Press.

Rössner, G. E. (1995). Odontologische und schädelanatomische Untersuchungen an *Procervulus* (Cervidae, Mammalia). *Münchner Geowissenschaftliche Abhandlungen*, *29*, 1–127.

Rössner, G. E. (1997). Bicohronology of ruminant assemblages in the Lower Miocene of Southern Germany. In J.-P. Aguilar, S. Legendre, & J. Michaux (Eds.), *Actes du Congrès BiochroM'97. Mémoires et Travaux de l'Ecole pratique de Hautes-Ètudes*. (pp. 609–618). Institut de Montpellier.

Rössner. G. E. (2004). Community structure and regional patterns in late early to middle Miocene Ruminantia of Central Europe. *Courier Forschungsinstitut Senckenberg*, *249*, 91–100.

Rössner, G. E., Bärmann, E. V., Heckeberg, N. S., Asher, R. J., Erpenbeck, D., & Wörheide, G. (2013). On the phylogenetic position of the hornless pecoran *Amphimoschus* – an example of arising challenges with the incorporation of fossils in extant combined frameworks. *Zitteliana*, *31*, 30–31.

Sánchez, I. M., Abbas, S. G., Khan, M. A., Babar, M. A., Quiralte, V., & DeMiguel, D. (2022). The first Asian record of the mouse-deer *Afrotragulus* (Ruminantia, Tragulidae) reassess its evolutionary history and offers insights on the influence of body weight on *Afrotragulus* diversification. *Historical Biology*, https://doi.org/10.1080/08912963.2022.2050719

Sánchez, I. M., Cantalapiedra, J. L., Ríos, M., & Morales, J. (2015). Systematics and evolution of the Miocene three-horned palaeomerycid ruminants (Mammalia, Cetartiodactyla). *PLOS ONE*, *10(*12*)*, e0143034. https://doi.org/10.1371/journal.pone.0143034

Sánchez, I. M., Domingo, M. S., & Morales, J. (2010). The genus *Hispanomeryx* (Mammalia, Ruminantia, Moschidae) and its bearing on musk deer phylogeny and systematics. *Palaeontology*, *53*, 1023–1047. https://doi.org/10.1111/j.1475-4983.2010.00992.x

Sánchez, I. M., & Morales, J. (2008). *Micromeryx azanzae* sp. nov. (Ruminantia: Moschidae) from the Middle–Upper Miocene of Spain, and the first description of the cranium of *Micromeryx*. *Journal of Vertebrate Paleontology*, *28*, 873–885. https://doi.org/10.1671/0272-4634(2008)28[873:MASNRM]2.0.CO;2

Sánchez, I. M., Quiralte, V., Ríos, M., Morales, J., & Pickford, M. (2015). First African record of the Miocene Asian mouse-deer *Siamotragulus* (Mammalia, Ruminantia, Tragulidae): Implications for the phylogeny and evolutionary history of the advanced selenodont tragulids. *Journal of Systematic Palaeontology*, *13*, 543–556, https://doi.org/10.1080/14772019.2014.930526

Scopoli, J. A. (1777). *Introdvctio ad historiam natvralem sistens genera lapidvm, plantarvm, et animalivm hactenvs detecta, caracteribvs essentialibvs donata, in tribvs divisa, svbinde ad leges natvrae*. Pragae.

Scott, K. M. 1990. Postcranial dimensions of ungulates as predictors of body mass. In J. Damuth, & B. J. MacFadden (Eds.), *Body size in mammalian paleobiology* (pp. 301–336). Cambridge University Press.

Scott, K. M., & Janis, C. M. (1987). Phylogenetic relationships of the Cervidae, and the case for a superfamily 'Cervoidea'. In C. M. Wemmer (Ed.), *Biology and management of the Cervidae* (577 pp.). Smithsonian Institution Press.

Simpson, G. G. (1931). A new classification of mammals. *Bulletin of the American Museum of Natural History*, *59*, 259–293.

Solounias, N. (2007). Family Bovidae. In D. R. Prothero & S. E. Foss (Eds.), *The evolution of artiodactyls* (pp. 287–291). The Johns Hopkins University Press.

Stehlin, H. G. (1925). Catalogue des ossements de mammifères Tertiaires de la collection Bourgeois. *Bulletin de la société d'Histoire naturelle et d'anthropologie de Loir-et-Cher*, *18*, 77–277.

Stirton, R. A. (1944). Comments on the relationships of the Palaeomerycidae. *American Journal of Science*, *242*, 633–655. https://doi.org/10.2475/ajs.242.12.633

Wang, X.-M., Li, Q., Qiu, Z.-D., Xie, G.-P., Wang, B.-Y., Qiu, Z.-X., Tseng, Z. J., Takeuchi, G. T., & Deng, T. (2013). Neogene mammalian biostratigraphy and geochronology of the Tibetan Plateau. In X.-M. Wang, L. J. Flynn, & M. Fortelius (Eds.), *Fossil mammals of Asia: Neogene biostratigraphy and chronology*. (pp. 274–292). Columbia University Press.

Wang, X.-M., Wang, B.-Y., & Qiu, Z.-X. (2008). Early explorations of Tabenbuluk Region (Western Gansu Province) by Birger–Bohlin-reconciling classic vertebrate fossil localities with modern stratigraphy. *Vertebrata PalAsiatica*, *46*, 1–19.

Wang, X.-M., Wang, B.-Y., Qiu, Z.-X., Xie, G., Xie, J.-Y., Downs, W., Qiu, Z.-D., & Deng, T. (2003). Danghe area (Western Gansu, China) biostratigraphy and implications for depositional history and tectonics of Northern Tibetan Plateau. *Earth and Planetary Science Letters*, *208*, 253–269. https://doi.org/10.1016/S0012-821X(03)00047-5

Wang, Y., Zhang, Ch., Wang, N., Li, Z., Heller, R., Liu, R., Zhao, Y., Han, J.-P., Pan, X.-Y., Zhuqing Zheng, X., Dai, X., Chen, C., Dou, M., Peng, S., Chen, X., Liu, J., Li, M., Wang, K., Liu, Ch., … Qiu, Q. (2019). Genetic basis of ruminant headgear and rapid antler regeneration. *Science*, *364*, eaav6335. https://doi.org/10.1126/science.aav6335

Webb, S. D., & Taylor, B. E. (1980). The phylogeny of hornless ruminants and a description of the cranium of *Archaeomeryx*. *Bulletin of the American Museum of Natural History*, *167*, 121–157.

Zachos, J., Pagani, M., Sloan, L., Thomas, E., & Billups, K. (2001). Trends, rythms, and aberrations in global climate 65 Ma to present. *Science*, *292*, 686–693. https://doi.org/10.1126/science.1059412

Associate Editor: Guillaume Billet